# Black hole mass estimates from high-ionization lines: breaking a taboo?

Paola Marziani[1]

in collaboration with

D. Dultzin[3], A. Negrete[3], A. del Olmo[2], M. A. Martínez-Carballo[2], M. L. Martínez-Aldama[2], G. M. Stirpe[4], E. Bon[5], N. Bon[5], M. D'Onofrio[6]

*[1]INAF - Osservatorio Astronomico di Padova, Padova, Italia*
*[2]Instituto de Astrofísica de Andalucía (CSIC), Granada, España*
*[3]Instituto de Astronomía, UNAM, México, D.F., México*
*[4]INAF - Osservatorio Astronomico di Bologna, Bologna, Italia*
*[5]Astronomska Opservatorija, Beograd, Serbia*
*[6]Dipartimento di Fisica ed Astronomia "Galileo Galilei", U. di Padova, Padova, Italia*

# Summary

Introduction:  importance of black hole mass estimates

Black hole mass ($M_{\rm BH}$) estimates: the virial assumption

The “rehabilitating” power of E1

Virial broadening estimators from:

a) Low ionization lines (LILs, IP < 15 eV: Hβ, MgII 2800)

b) High ionization lines  (HILs, IP > 40 eV: CIVλ1549)

c) Intermediate ionization lines (IILs: SiIII]λ1892, Al IIIλ1860); preliminary results

“Photoionization masses”

Conclusion

# Importance of black hole mass determination

**Feedback to the host galaxy**: massive, fast outflows are affected by the ratio of radiation to gravitational forces, and are invoked to account for the $M_{BH}$ - bulge velocity dispersion correlation

Fabian 2012; Kormendy & Richstone 2013: King & Pounds 2015, Ferland et al. 2009; Marziani et al. 2016a,b; 2017 (submitted)

The ratio between radiation and gravitation forces: influences **broad-line region dynamics**; lower column density material may flow out of the emitting region

Ferland et al. 2009; Marziani et al. 2010; Netzer & Marziani 2010; Marziani et al. 2017, submitted.

**Black hole masses of high redshift quasars** provide constraints on primordial black holes collapse

Smith, Broom, Loeb 2017, and references therein; Trakhtenbrot et al. 2015

# Black hole masses: the virial assumption

$$M_{\mathrm{BH}} = \frac{f r (\delta v)^2}{G}$$

geometry
dynamics

$r_{\mathrm{BLR}}$

FWHM
σ
FWZI

## *f* structure factor

$$\text{if } \delta v = \mathrm{FWHM}, \text{isotropy} : \frac{\sqrt{3}}{2}\mathrm{FWHM} \rightarrow f = 0.75$$

## δv : virial broadening

estimators from line width measurements

Key assumption: emission line (or component) symmetric and unshifted with respect to the quasar rest frame

## Emitting region distance $r_{\mathrm{BLR}}$

from central continuum source

Time lag τ given by the peak or centroid of the cross-correlation function between line and continuum ($r_{\mathrm{BLR}} = c\,\tau$); scaling laws, or photoionization estimates

# Virial black hole masses: scaling laws for large samples

***r*$_{BLR}$ primary**: $r_{BLR} = c\,\tau_{H\beta}$
from Hβ reverberation mapping:
available for ~100 mainly low-*z* (<1), type 1 AGN

(e.g., Kaspi et al., Bentz. et al. 2009, Du et al. 2016)

***r*$_{BLR}$ secondary**: scaling laws for large samples: $r \propto L^a$, $a \approx 0.5$

(Kaspi et al. 2000; Bentz et al. 2006)

**Mass scaling laws:**

$M_{BH} = M_{BH}(L, \mathrm{FWHM})$

$M_{BH} = kL^a FWHM^b$

$a \approx 0.5$, b≈2 (virial)

(e.g., Vestergaard & Peterson 2006; Trakhtenbrot & Netzer 2012)

$a \neq 0.5$, b≠2

(e.g., Shen & Liu 2012; Park et al. 2013; Shen et al 2016)

$$\text{Eddington ratio} = \frac{L_{\rm bol}}{L_{\rm Edd}} \propto \frac{\lambda L_\lambda \times \mathrm{B.C.}}{M_{\rm BH}}$$

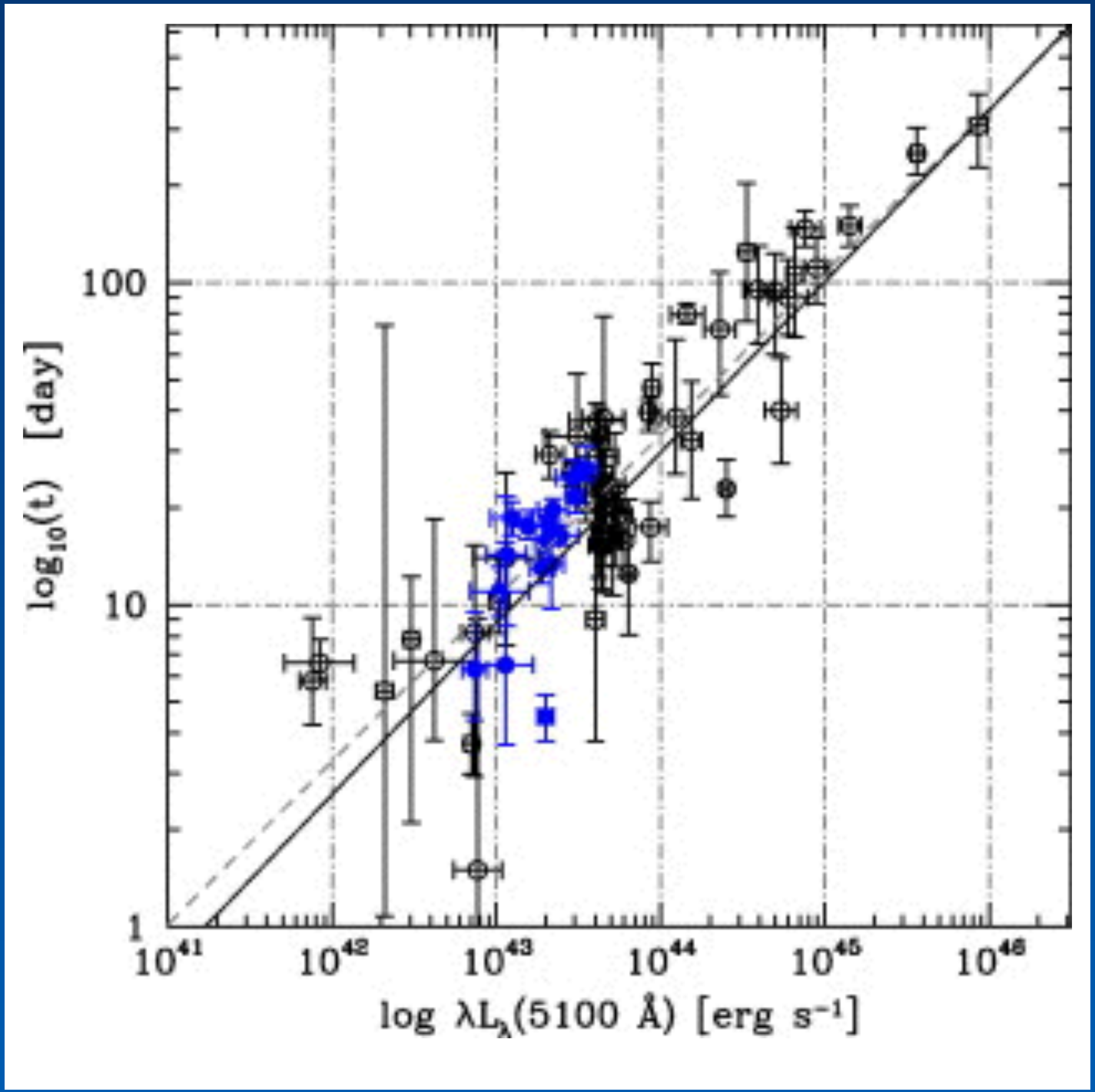


**The *M*$_{BH}$ scaling laws provides a simple recipe usable with single epoch spectra**

**Reverberation mapping assumptions** compact continuum source, fairly linear response.
Unpredicted behavior of NGC 5548 in 2014: shielding, optically thin gas, changing size of continuum source?

Horne et al. 2017; Pei et al. 2017; Fasnaugh et al 2016

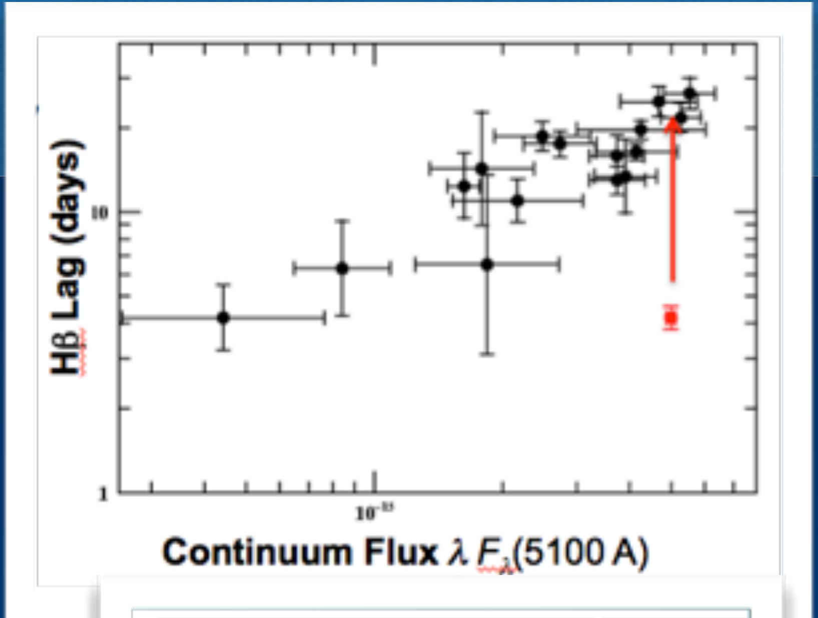


The **$r_{BLR}$ - L scaling relation**: has a non-negligible intrinsic dispersion, and $r_{BLR}$ depends on dimensionless accretion rate.

Du et al. 2016; 2017

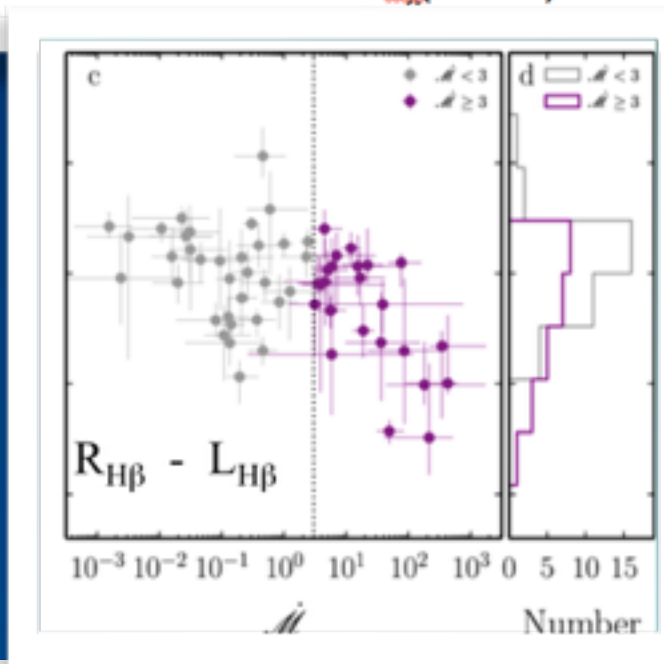


**Line profiles as virial broadening estimators:** errors so large to lead to full loss of information

e.g., Croom 2011

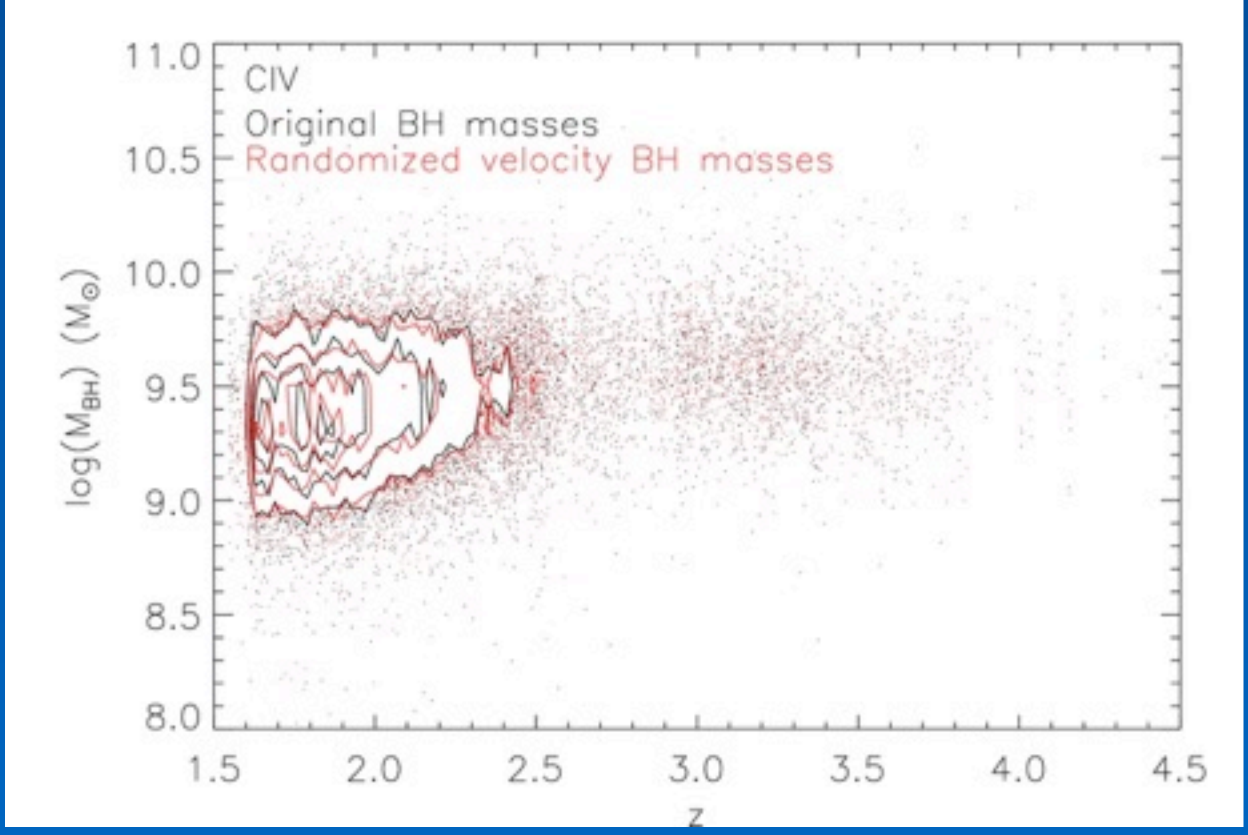


**One value of the structure factor** obtained scaling the $M_{BH}$ to agree with the dynamical masses, $f$(FWHM)≈2 but structure factor likely different for different type-1 quasar populations.

Woo et al. 2010; cf Gültekin et al. 2009;
Onken et al. 2004;
Ferrarere & Merritt 2000;
also Graham et al. 2011

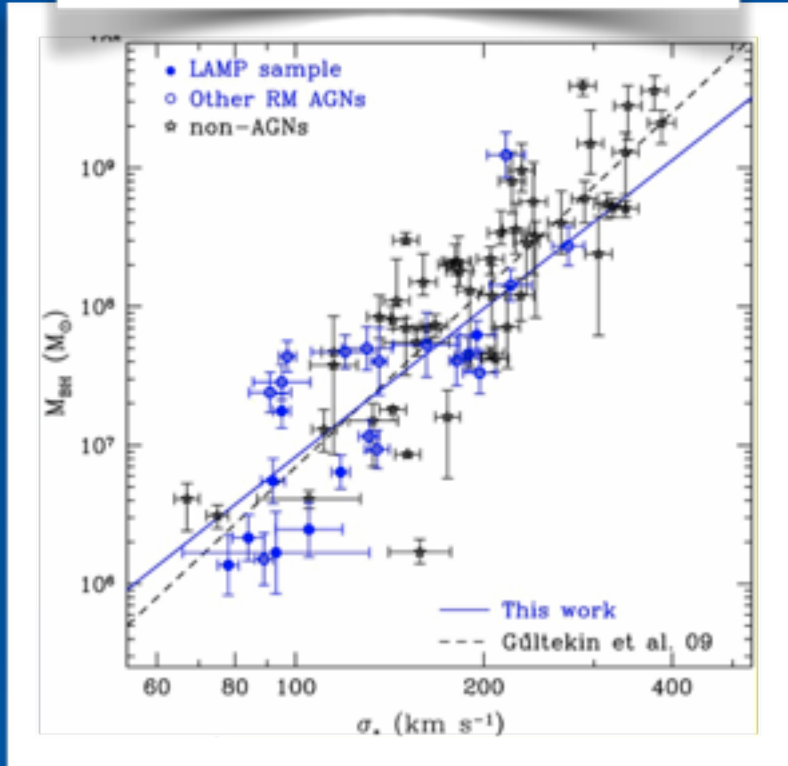

# The “rehabilitating power of Eigenvector 1”: The Quasar Main Sequence

## Eigenvector 1: an useful tool to organize quasar diversity

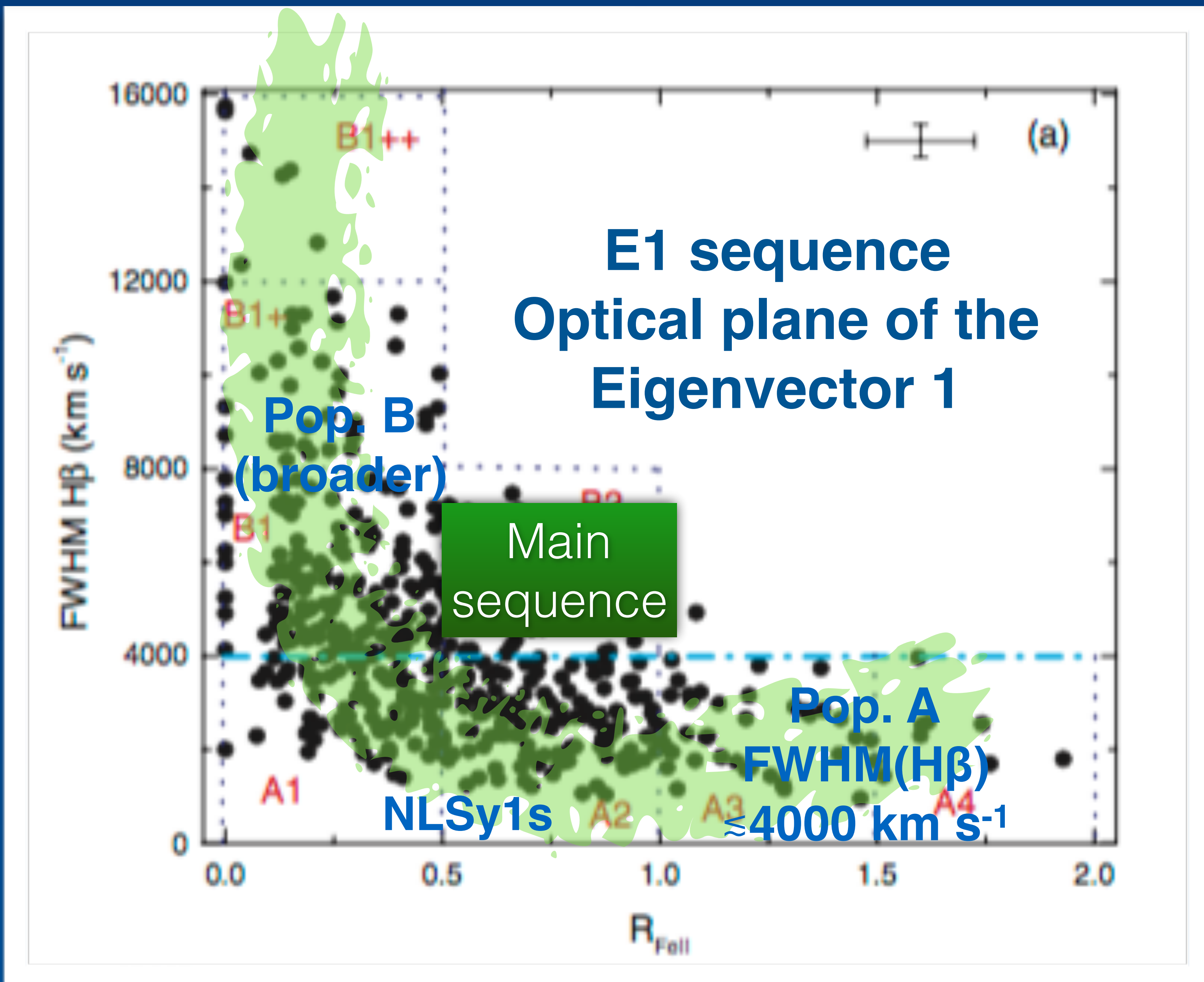


Sulentic et al. 2002 ($z < 1$, log L < 47 [erg/s]); **Boroson & Green 1992; Sulentic et al. 2000**, 2007; discussed in more than 400 papers: Dultzin-Hacyan et al. 1997; Shang et al. 2003, Yip et al.2004, Kruzcek et al 2011; Tang et al. 2012; Kuraszkiewicz et al. 2008; Mao et al. 2009; Grupe 2004, Wang et al. 2006 SDSS data : Richards et al. 2011; Shen & Ho 2014, Sun & Ho 2015, Brotherton et al. 2015

**Eigenvector 1**: Originally defined by a Principal Component Analysis of PG quasars, and associated with an anti-correlation between strength of FeIIλ4570, $R_{FeII}$ (or [OIII] 5007 peak intensity) and FWHM of Hβ.

The **E1 main sequence (MS) in the optical plane** FWHM(Hβ) vs $R_{FeII}$ = I(FeIIλ4570)/I(Hβ) allows for the **definition of spectral types.**

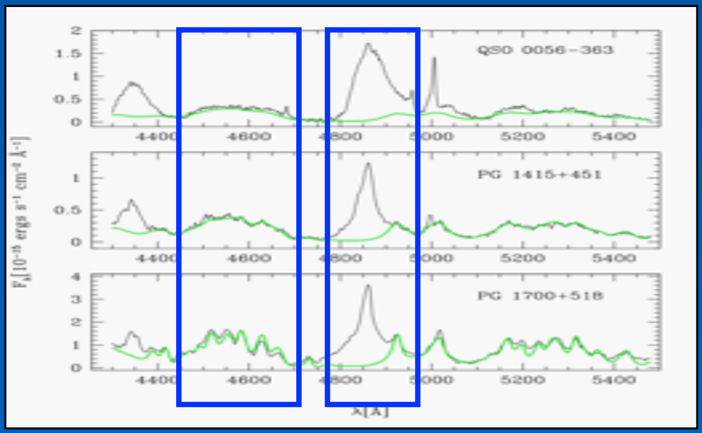


$$R_{\rm FeII} = \frac{I({\rm FeII}\lambda4570)}{I(H\beta)} \approx \frac{W({\rm FeII}\lambda4570)}{W(H\beta)}$$

## *L/L*$_{Edd}$ is the driver of the E1 MS

Boroson & Green 1992, Marziani et al. 2001, Shen &Ho 2014, Sun & HSen 2015

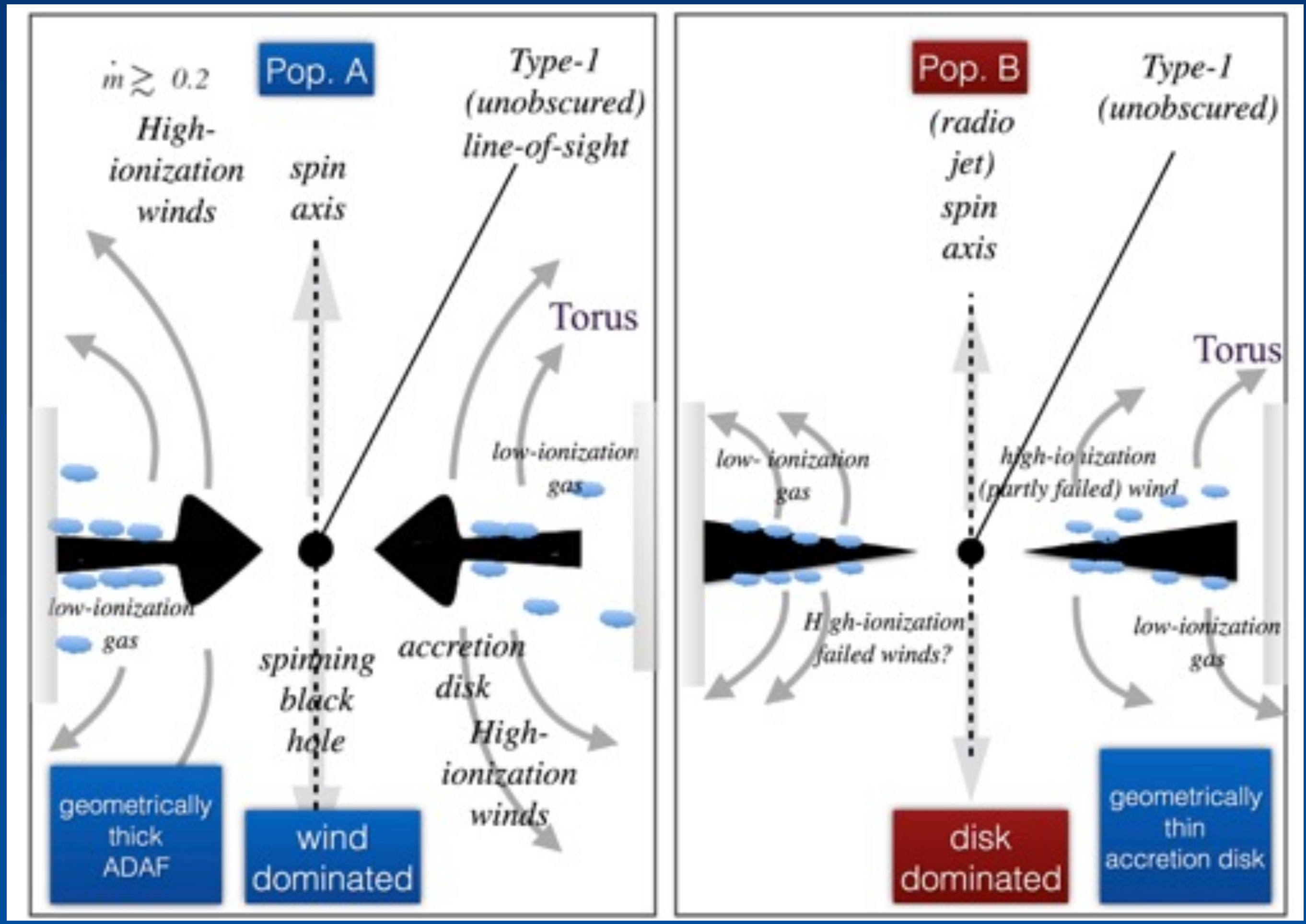


## Population A (FWHM Hβ<4000 km/s) and Population B(roader) sources

Pop. A: high L/L$_{EDD}$; Pop. B: low L/L$_{EDD}$.

More appropriate than the distinction NLSy1-rest of type-1 AGNs; called wind and disk dominated by Richards et al., Population 1 and 2 by Collin et al. 2006.

**Probably due to a change of accretion mode**

Marziani et al. 2003b, Marziani et al. 2014

**4DE1**: 2 more "ortogonal" parameters: $\Gamma_{soft}$, c(½) CIVλ1549;

many more correlates, including line profile shapes

Table 1s of Sulentic et al. 2011 and Fraix-Burnet et al. 2017

The 4D Eigenvector 1 space of quasars

| Observed parameter | Physical interpretation |
|---|---|
| $R_{FeII}$=I(FeII)/I(Hβ) | ionization degree *col. density, Z* |
| FWHM(Hβ) | velocity field of low-ionization gas |
| CIVλ1549 Shift | velocity field of high-ionization gas |
| $\Gamma_{soft}$ (0.2-2 KeV) | Compton thick / accretion disk emission? |

} Optical plane of 4DE1

# Virial broadening estimators: LILs along E1 sequence

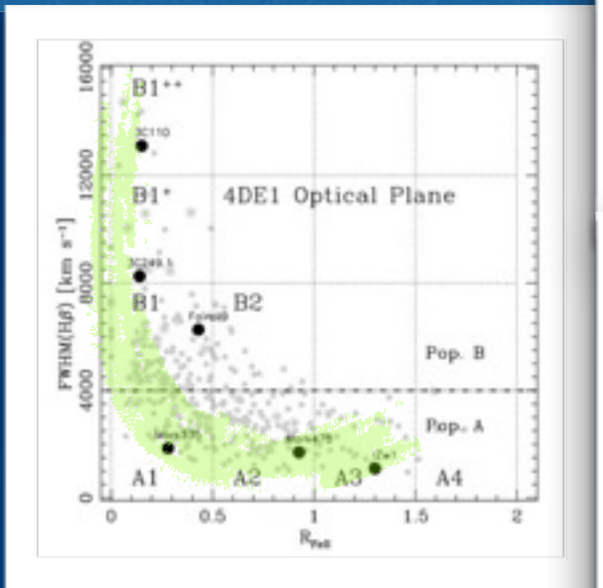


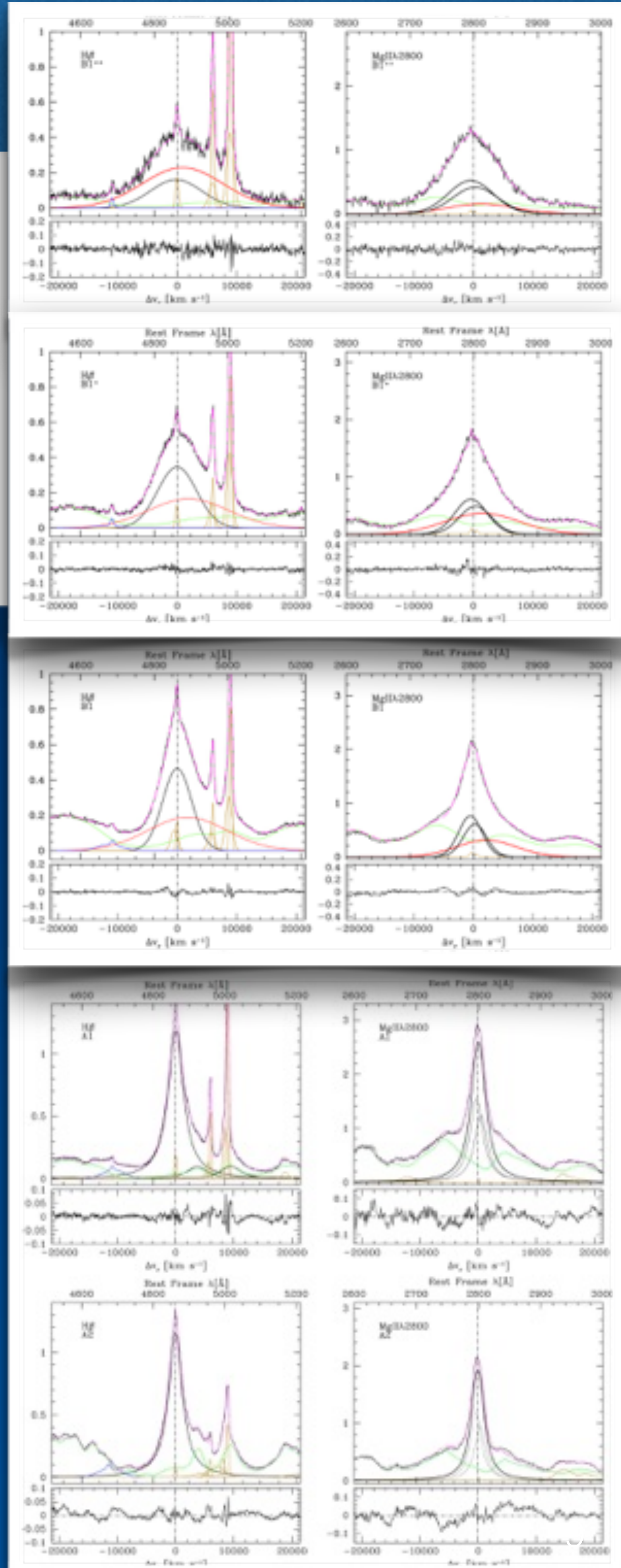

**Hβ and MgII**

from **extreme Pop. B**: low FeII, broad profiles

redward asymmetric

Broad component + (redshifted) very-broad component

to **extreme Pop. A,** narrower, strong FeII, slightly blueward asymmetric

Lorentzian profiles + blueshifted excess

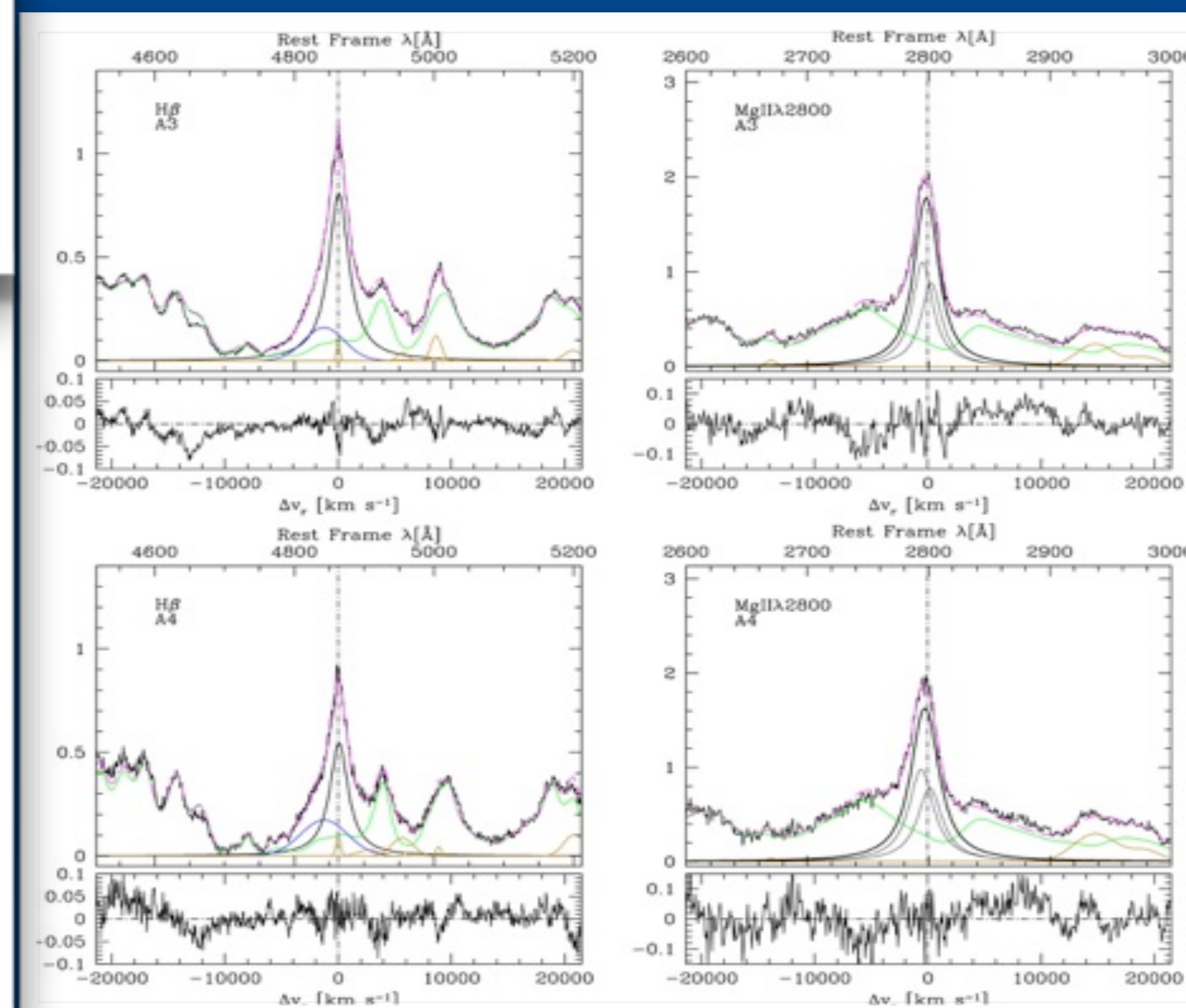


Marziani et al 2013a,b; SDSS sample covering both Hβ and MgII 0 .4 < z < 0.7

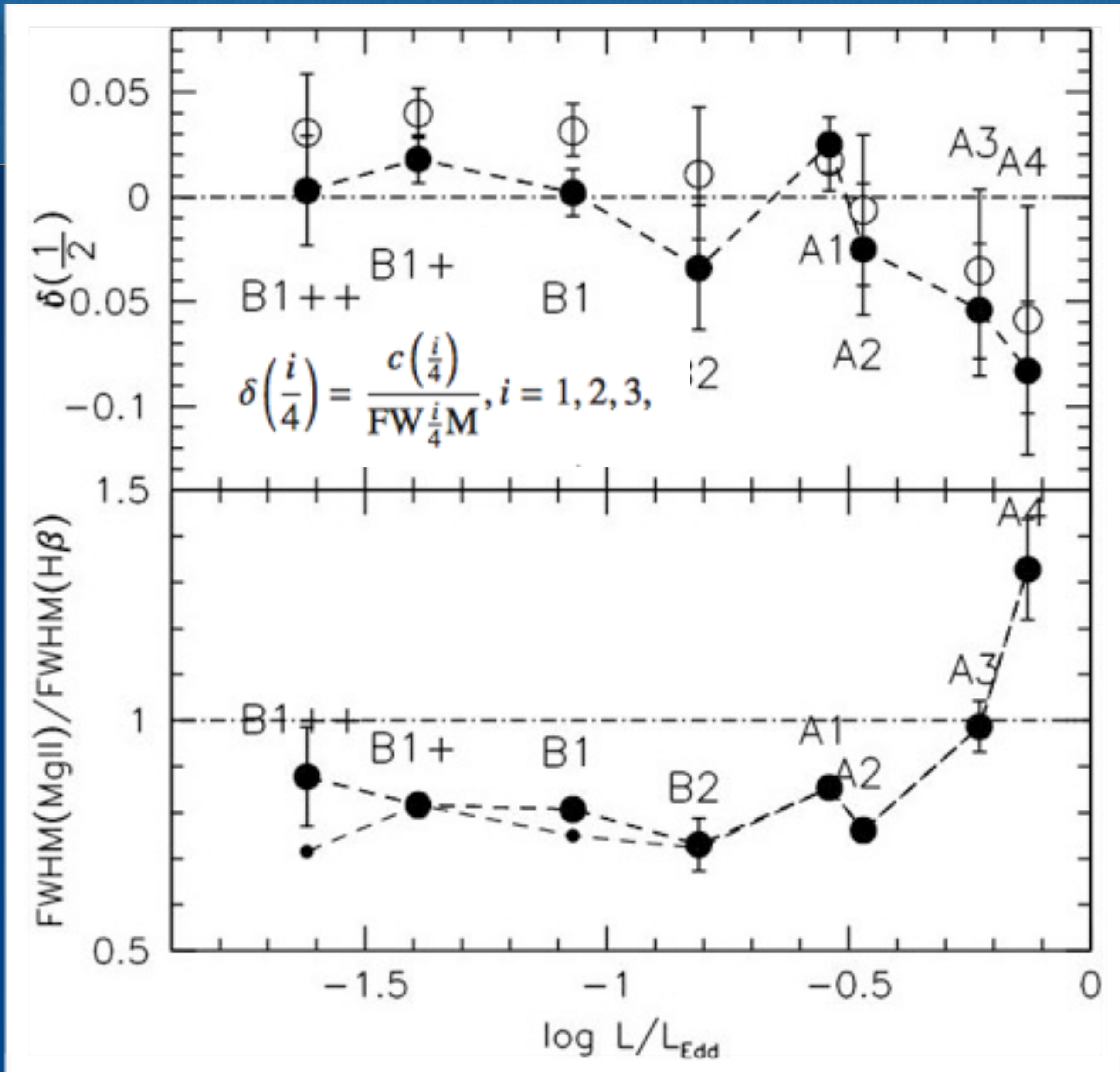


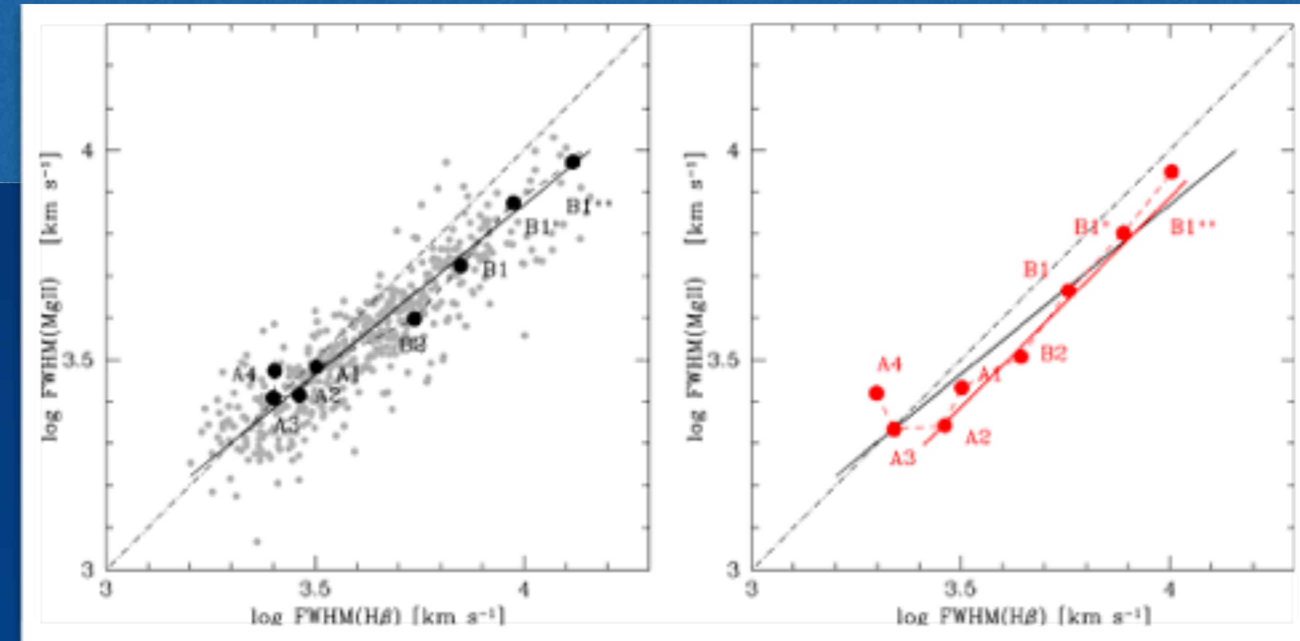


SDSS sample covering both Hβ and MgII 0 .4 < z <0.7; Marziani et al. 2013a,b; Wang et al. 2009; cf. Trakhtenbrot & Netzer 2012; Mejia-Restrepo et al. 2016

LIL resonance line MgIIλ2800: low ionization outflows detected in the extreme Pop. A spectral types

$$FWHM(\text{line})_{\text{vir}} = \xi FWHM(\text{line})_{\text{obs}}$$

where

$$\xi = \frac{FWHM(\text{line})_{\text{BC}}}{FWHM(\text{line})_{\text{obs}}},$$

LILs are dominated by a symmetric, “virialized” broad component: $1 \gtrsim \xi \gtrsim 0.75$.

| | $\xi_{H\beta}$ | $\xi_{MgII}$ |
|---|---|---|
| **A3-A4** | 0.8/0.9 | 0.75/0.8 |
| **A1-A2** | 1.0 | 1.0 |
| **B1** | 0.8 | 0.9 |
| **B1+/B1++** | 0.8 | 0.9 |

# Virial broadening estimators: the HIL CIVλ1549 along the E1 sequence

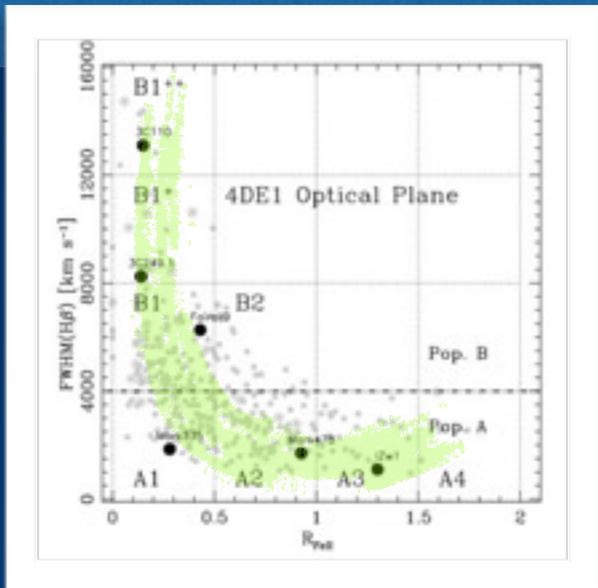


CIVλ1549: scaled Hβ from + excess blueshifted emission increasing from B1++ to A3

almost symmetric, unshifted LIL (⇒“virialized” emitting region) +

**outflow/wind component that dominates in A3/A4 spectral types**

e.g., Leighly 2000, Bachev et al. 2004, Marziani et al. 2010; Denney et al. 2012

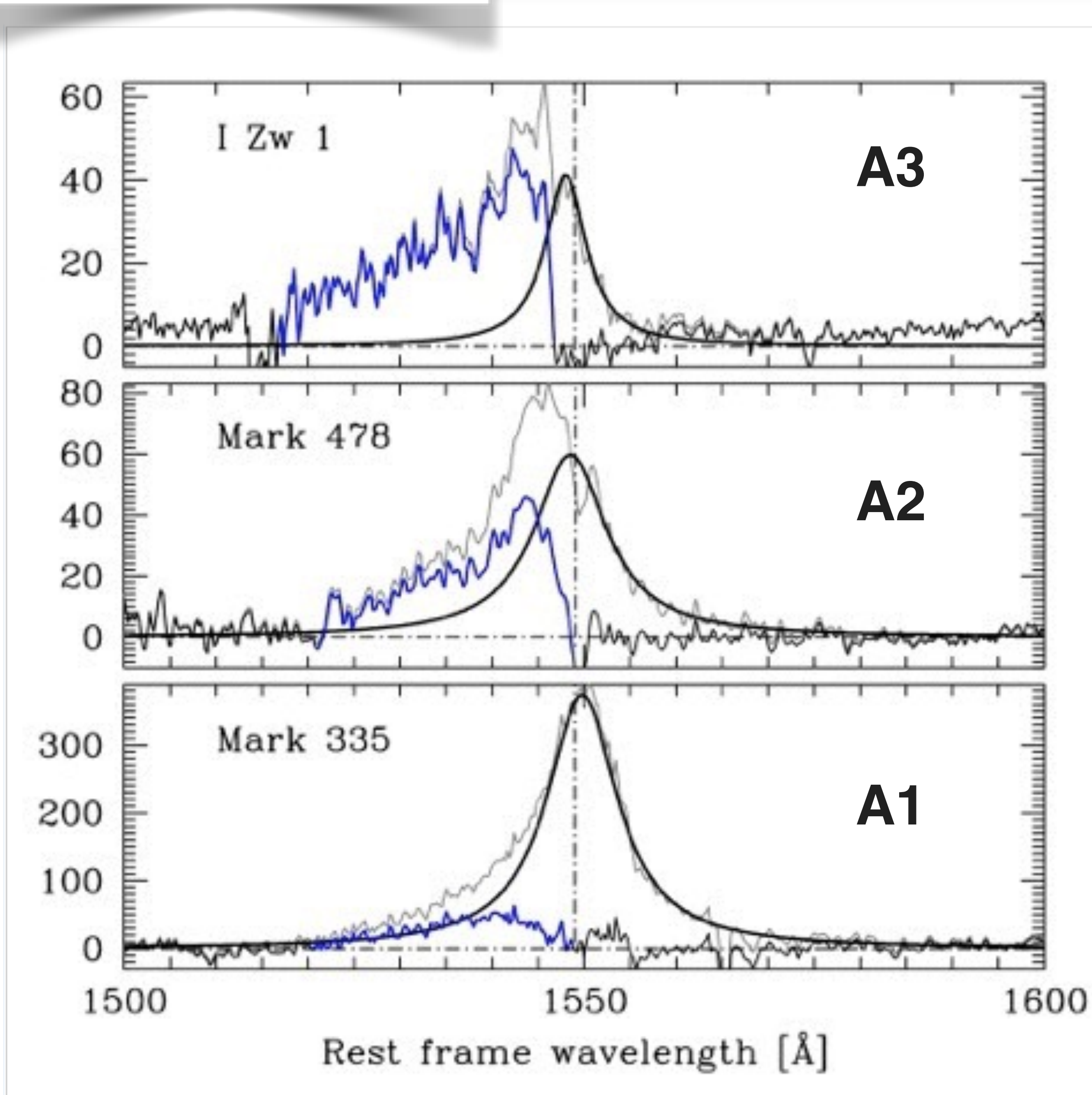


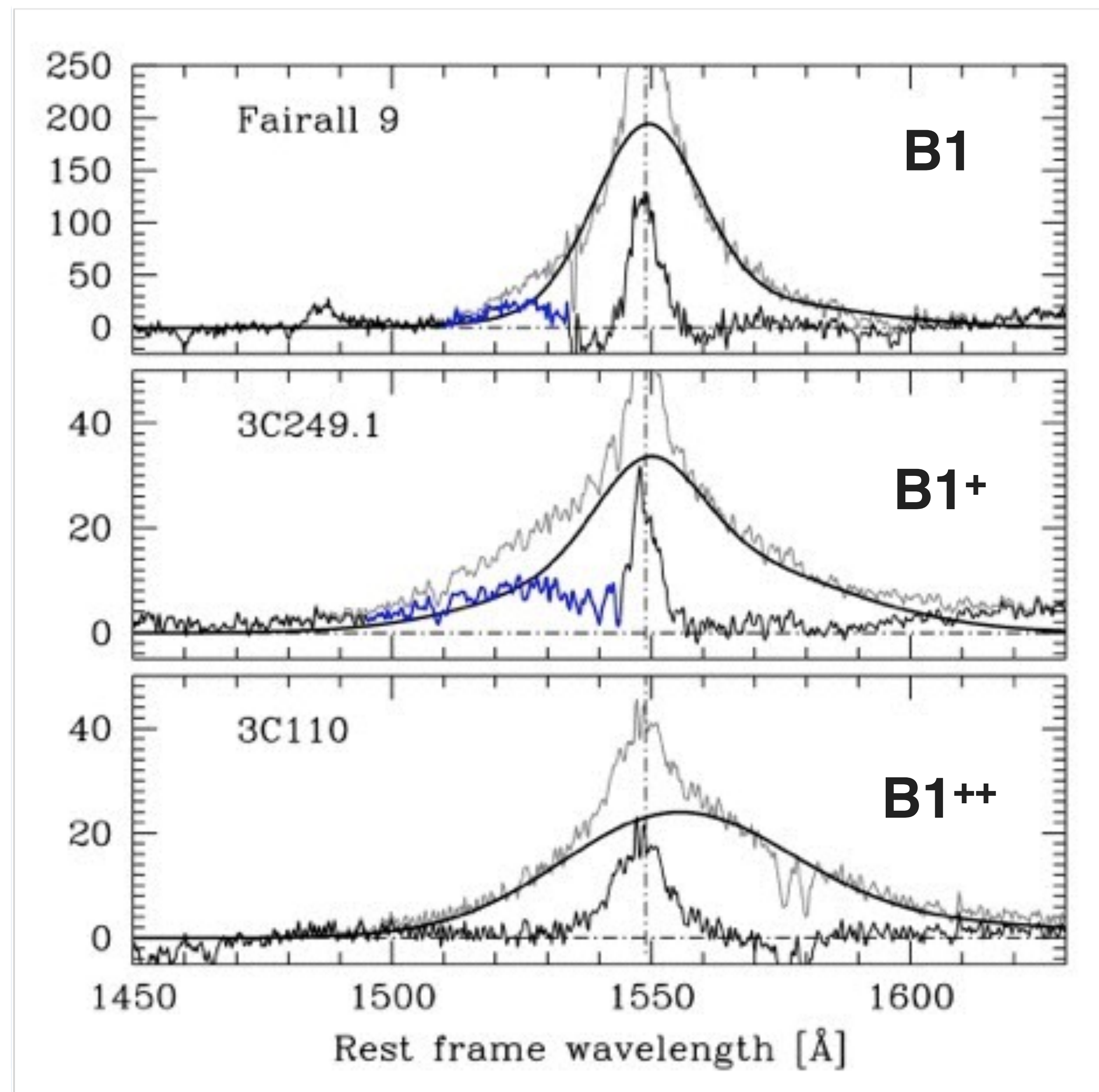

# Virial broadening estimators: the HIL CIVλ1549 along the E1 sequence

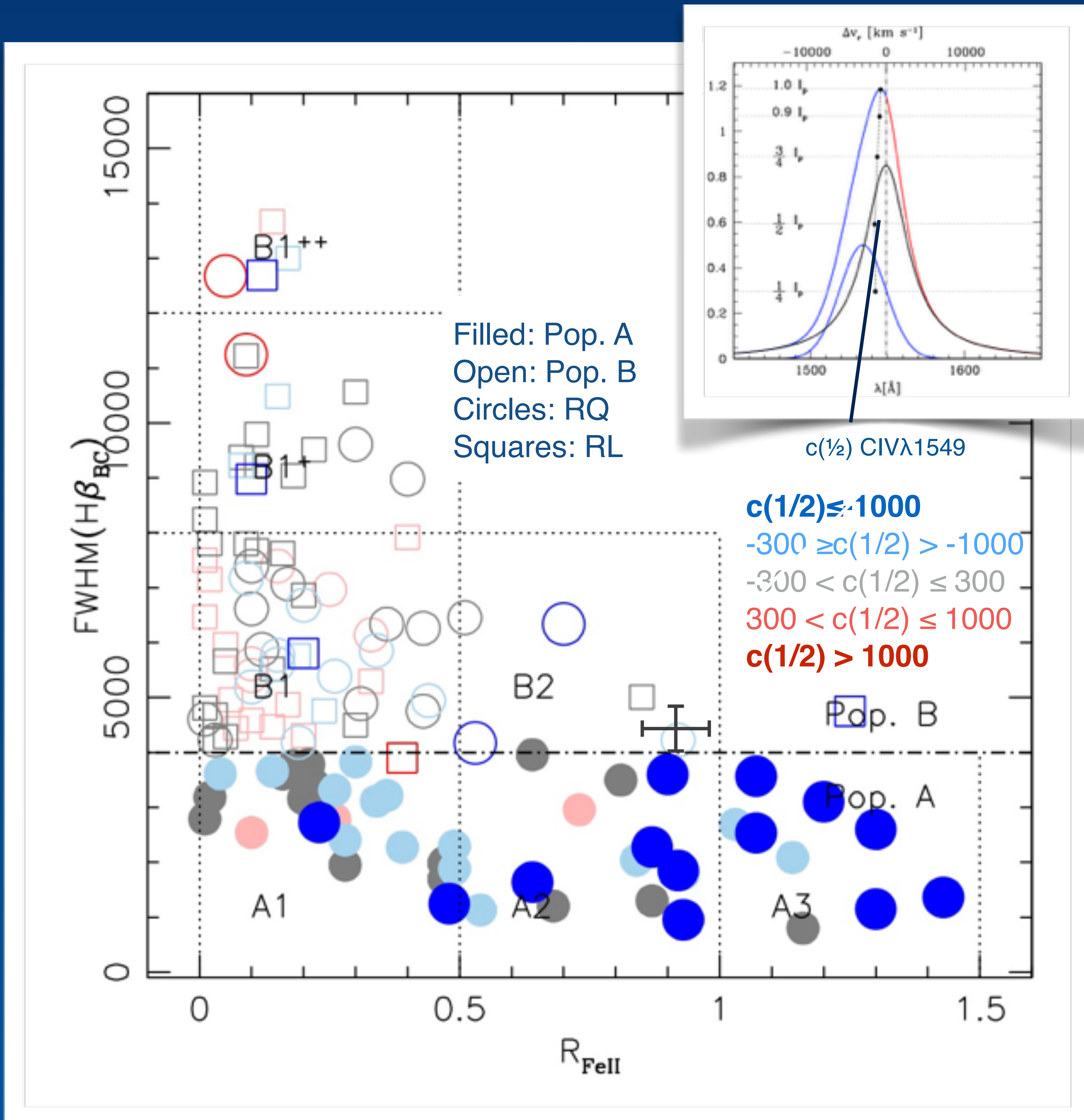


Large shift of CIVλ1549 centroid at ½ along the MS are found for FWHM(Hβ) < 4000 km s$^{-1}$ in the E1 optical plane.

This result also reinforces the suggestion of a discontinuity at FWHM(Hβ) ≈ 4000 km s$^{-1}$ suggested by the Hβ profile shape change.

Marziani & Sulentic 2012; Sulentic et al. 2007; low *z* sample UV FOS data

# Virial broadening estimators: the CIVλ1549 "taboo"

1. FWHM(Hβ) and $L_\lambda$(5100 Å): For the optical continuum luminosity and FWHM of the Hβ broad component,

$$\log M_{\rm BH}({\rm H}\beta) = \log\left\{\left[\frac{{\rm FWHM(H}\beta)}{1000\ {\rm km\ s^{-1}}}\right]^2\left[\frac{\lambda L_\lambda(5100\ \text{Å})}{10^{44}\ {\rm ergs\ s^{-1}}}\right]^{0.50}\right\} + (6.91 \pm 0.02). \quad (5)$$

$$\log M_{\rm BH}({\rm C\ IV}) = \log\left\{\left[\frac{{\rm FWHM(C\ IV)}}{1000\ {\rm km\ s^{-1}}}\right]^2\left[\frac{\lambda L_\lambda(1350\ \text{Å})}{10^{44}\ {\rm ergs\ s^{-1}}}\right]^{0.53}\right\} + (6.66 \pm 0.01). \quad (7)$$

Vestergaard & Peterson 2006; mass "taboo": Sulentic et al. 2007; Netzer et al. 2007

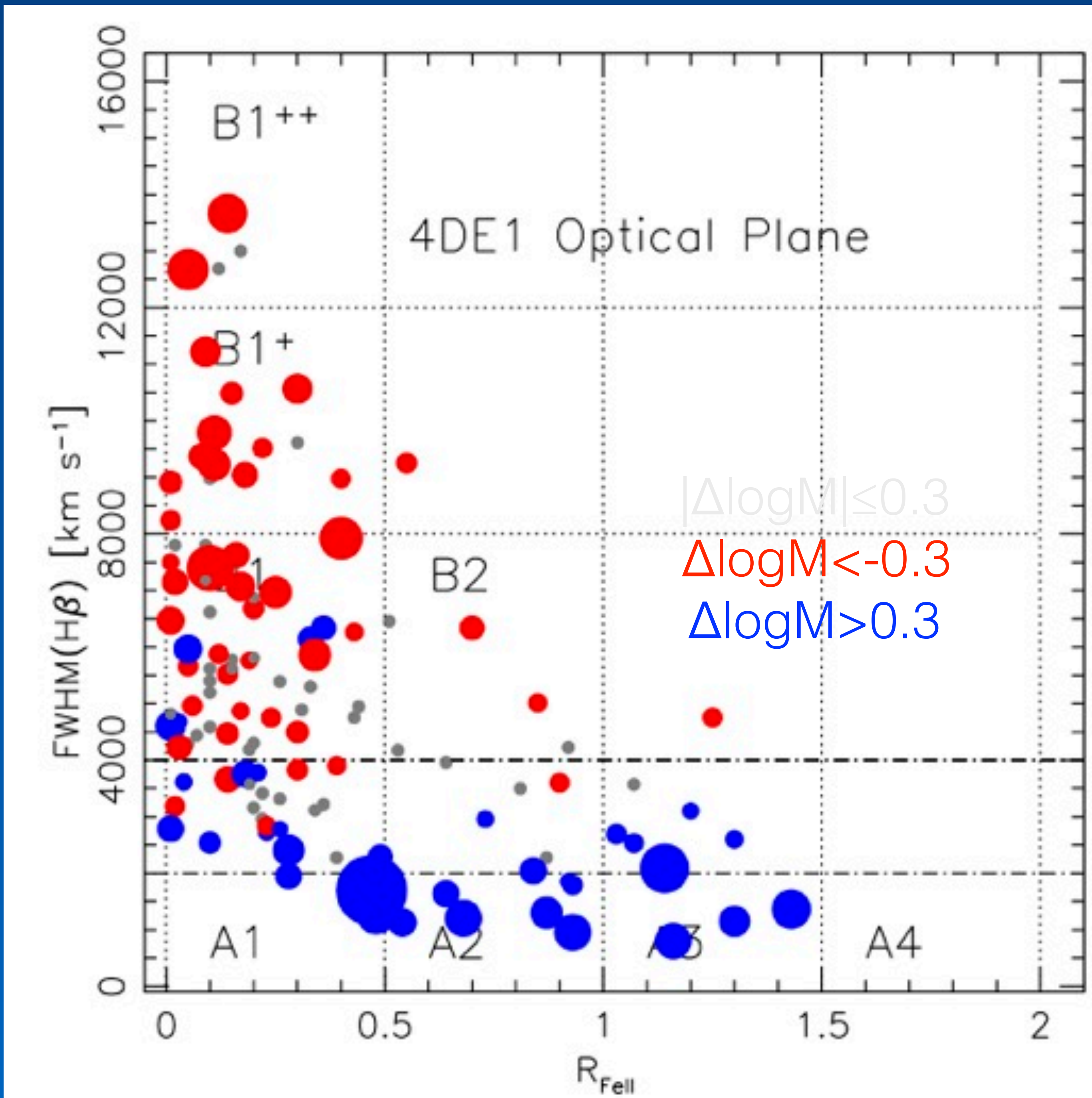


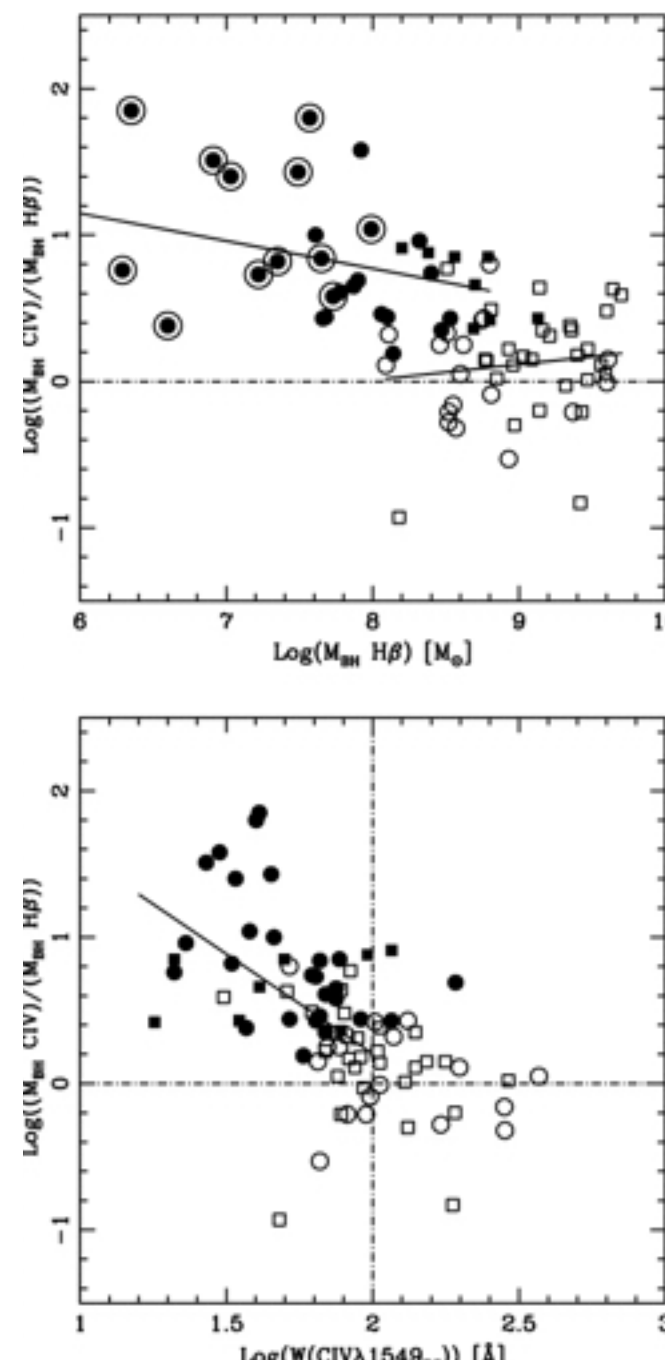


Scaling laws assumed that the width of CIV and Hβ are equivalent

**Bias along the E1 sequence, especially for Pop. A**

errors as large as 2 dex.

Pop. A sources are more frequently selected at high z, high L

# Virial broadening estimators: LIL Hβ behavior over a wide luminosity range

Composite spectra: Hβ becomes broader with increasing *L* (over 43 < logL < 48.5 [erg $s^{-1}$]) but shapes are similar to the ones at low z

Pop. A Pop. B

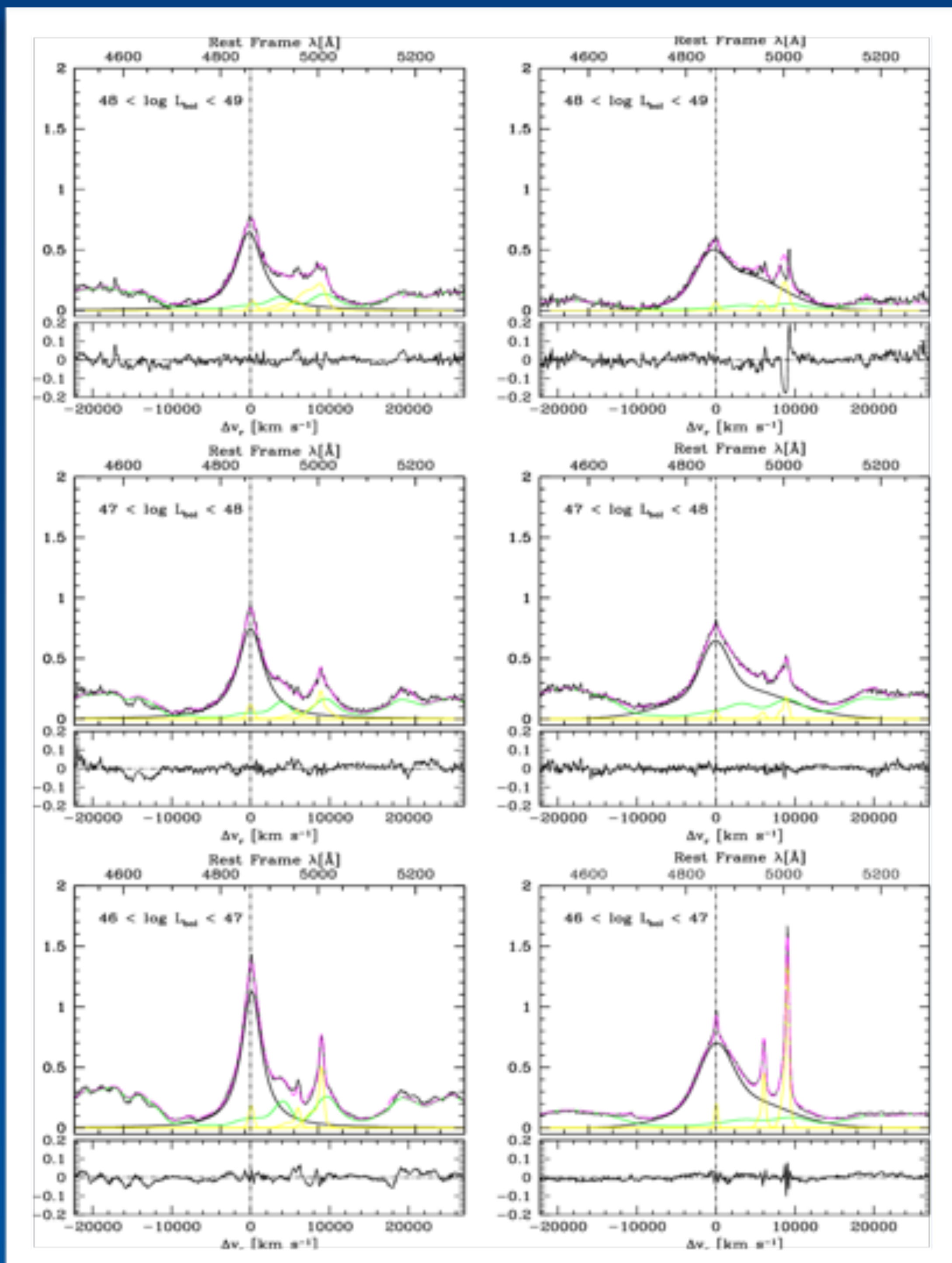


Pop. A Pop. B

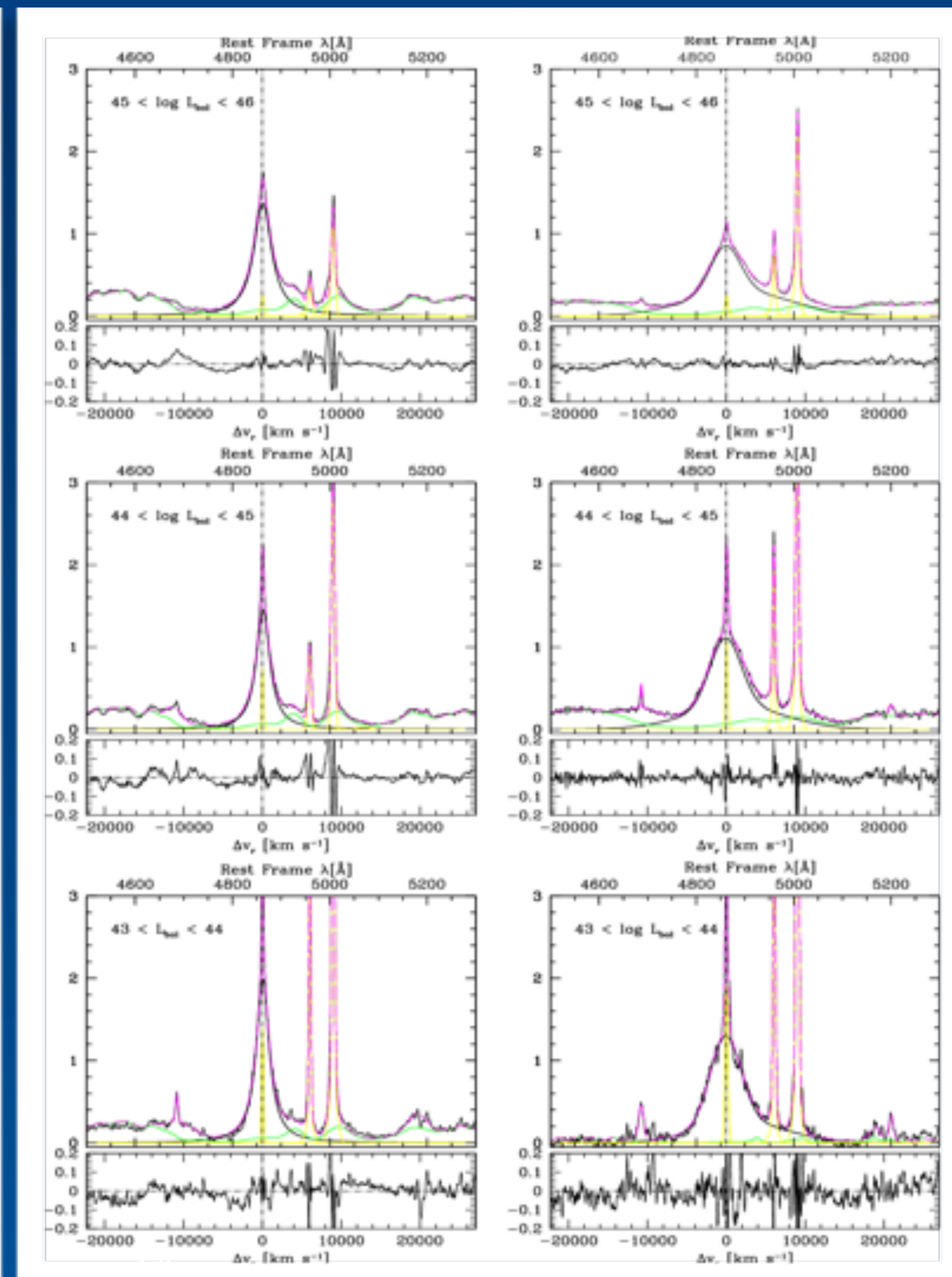


**The Pop. A / Pop. B differences are preserved at high L**

HE/ISAAC high-L sample (52 sources) + SDSS continuum subtracted spectra

Marziani et al. 2009; Zamfir et al. 2010

# Virial broadening estimators: LIL Hβ at high-L

“Symmetrization” methods:

- substitution of the BC extracted through the `specfit` analysis in place of the full Hβ profile.
- symmetrization of the profile: $\mathrm{FWHM_{symm}} = \mathrm{FWHM} - 2\,c(\frac{1}{2})$ (symm in Fig. 2);
- correction based on spectral type, as defined from the analysis of the Hβ profile in a large SDSS-based sample at $0.4 \lesssim z \lesssim 0.7$ (labeled as cm in Fig. 2), following Marziani et al. (2013a). In practice, this means to correct Hβ for Pop. B sources by a factor $\xi_{\mathrm{H}\beta} \approx 0.8$;
- correction derived by pairing the observed FWHM to the best width estimator from reverberation mapping, following the relation $\mathrm{FWHM_c} \approx 1.14\,\mathrm{FWHM} - 601 - 0.0000217\mathrm{FWHM}^2$ derived by Sulentic et al. (2006, labeled `corr`);

All “symmetrization” methods could be considered equivalent at high L.

The Hβ profile shapes at high L are consistent with those at low-z, lower L.

**A “virialized system” emitting mainly LILs**

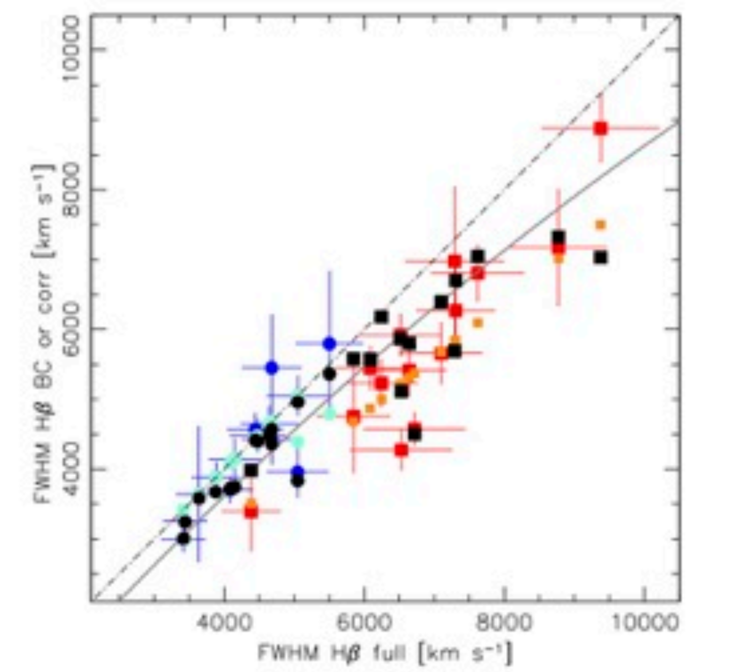


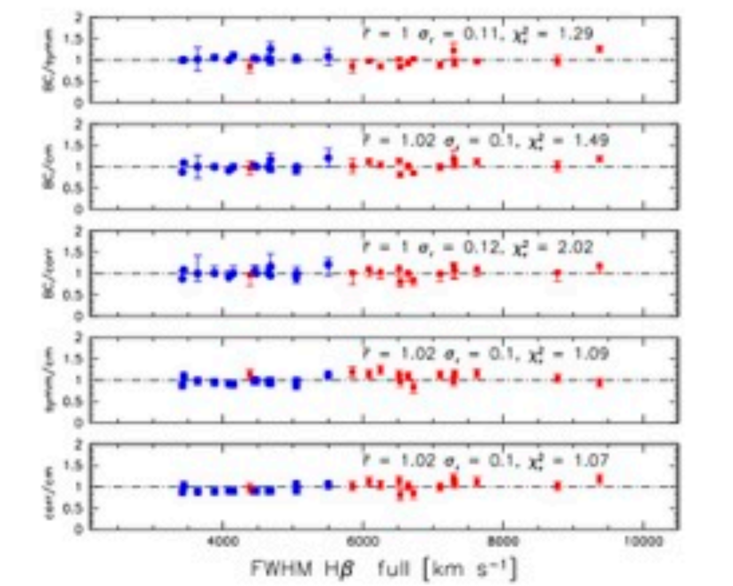


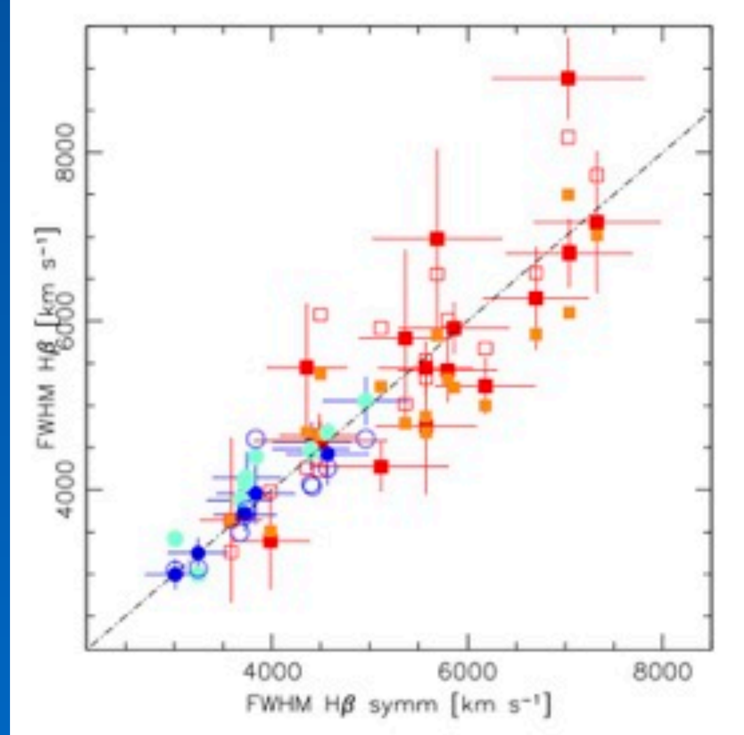

# Virial broadening estimators: LIL Hβ behavior over a wide luminosity range

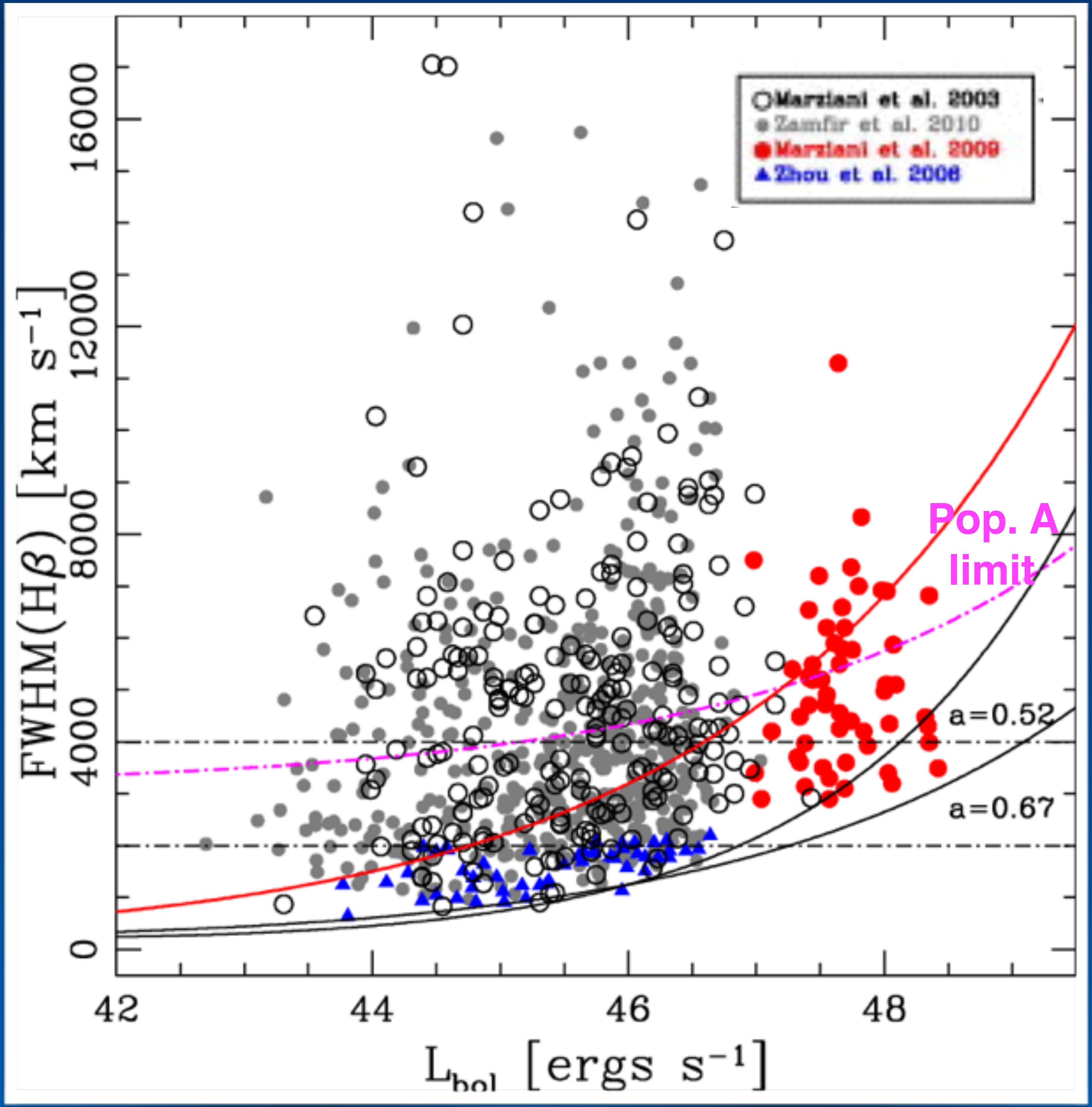


Minimum FWHM(Hβ) is luminosity-dependent, consistent with virial assumption.

The Pop. A limit is also luminosity dependent.

Curves assume the virial relation and $r_{BLR}$ scaling with luminosity:

$$r_{BLR} FWHM^2 \propto M$$

$$r_{BLR} \propto L^a$$

$$FWHM \propto (L/M)^{-1} L^{((1-2a)/2)}$$

Minimum FWHM is obtained for a limiting Eddington ratio ~ 1.



Marziani et al. 2009

# Virial broadening estimators: CIVλ1549 at high luminosity

High-L (≳$10^{47}$ erg $s^{-1}$, 1 <z<2) :
VLT/FORS HE sample (Sulentic et al 2017; CIV, 28 objects)
∩
VLT/ISAAC HE sample (Marziani et al. 2009, 52 objects)

median 3000 km $s^{-1}$ for Pop. A; 2 cases with CIV c(1/2) blueshift amplitude larger than 5000 km $s^{-1}$

**Widespread powerful outflows coexisting with a virialized low-ionization component**

## L>$10^{47}$ erg $s^{-1}$: high amplitude CIV 1549 blueshifts in both Pop. A and B

Sulentic et al., 2017

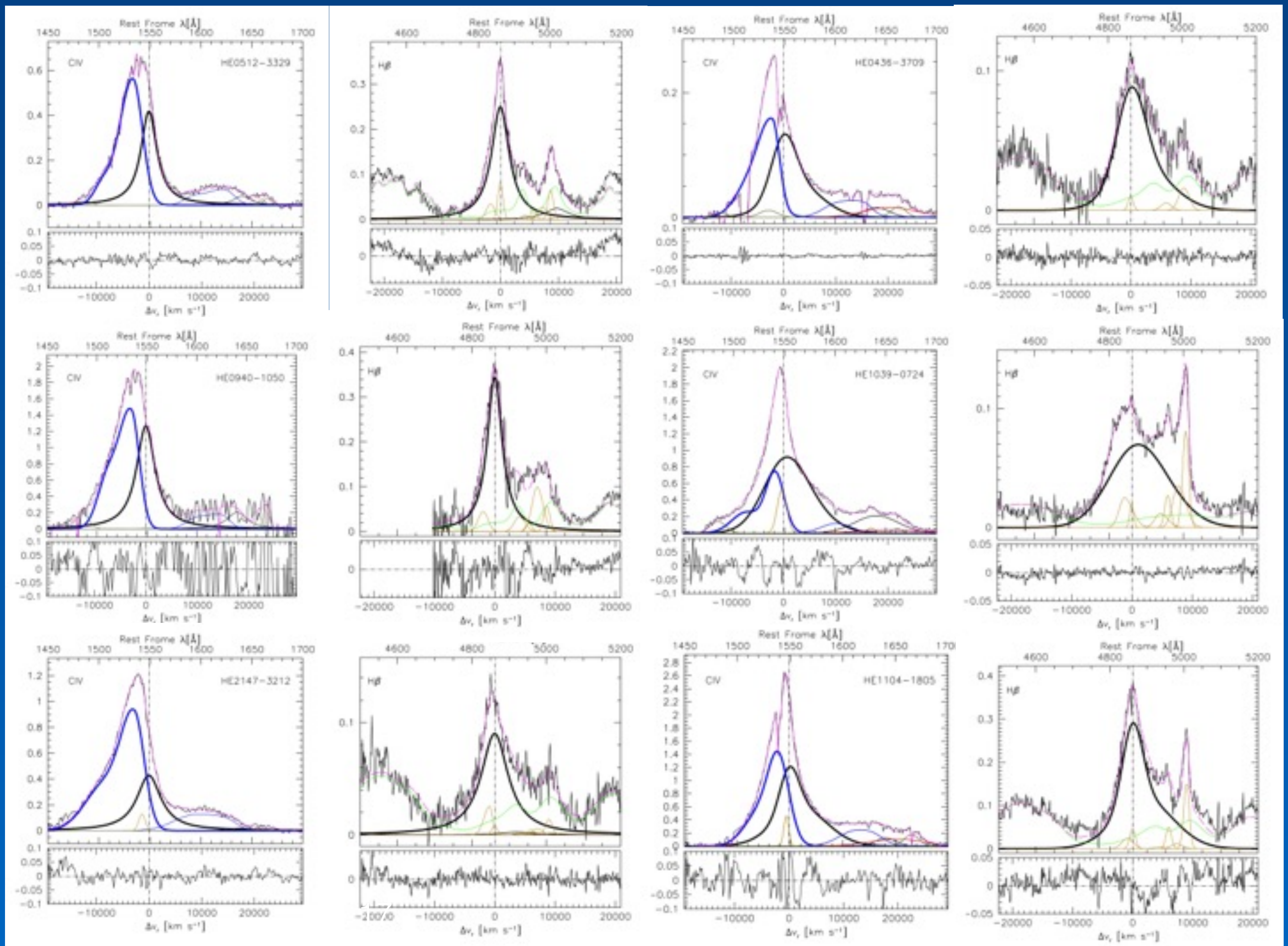

# Virial broadening estimators: LIL Hβ at high-L

Higher luminosity implies a **displacement of the MS** toward larger FWHM(Hβ) i.e., larger masses

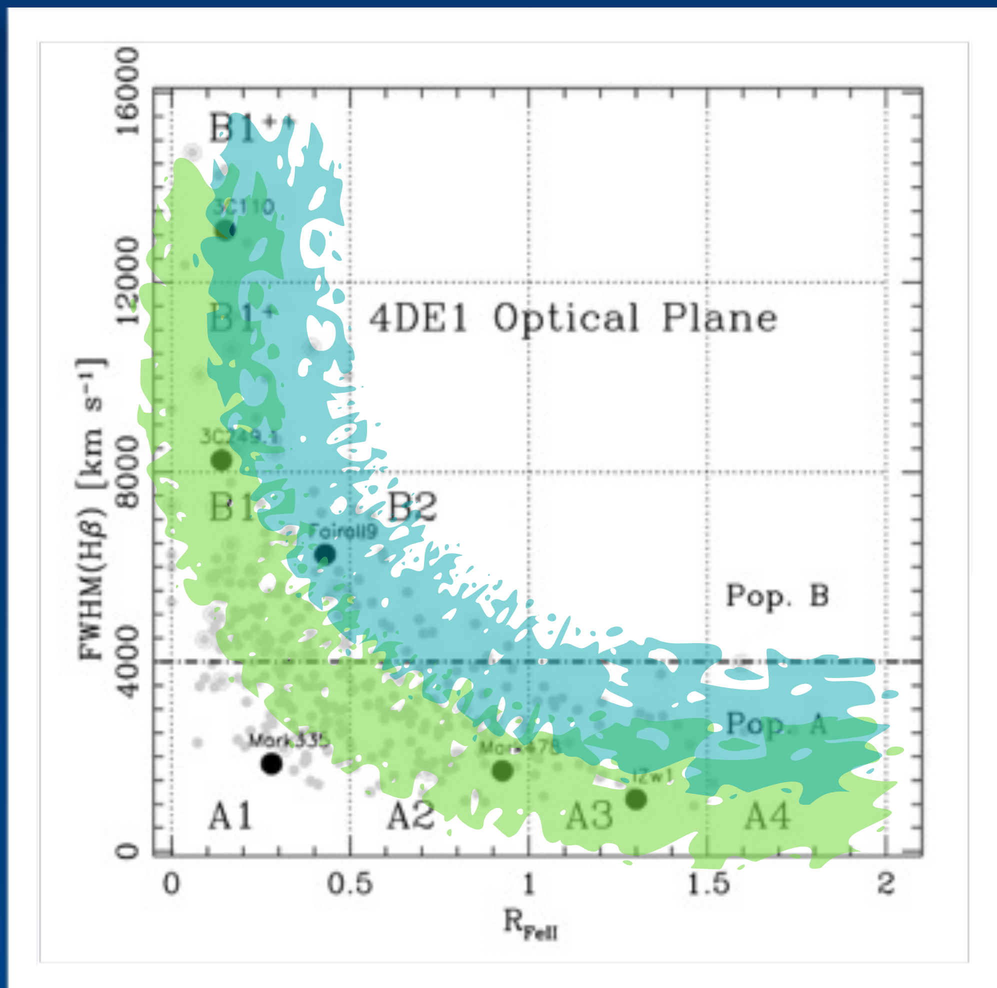


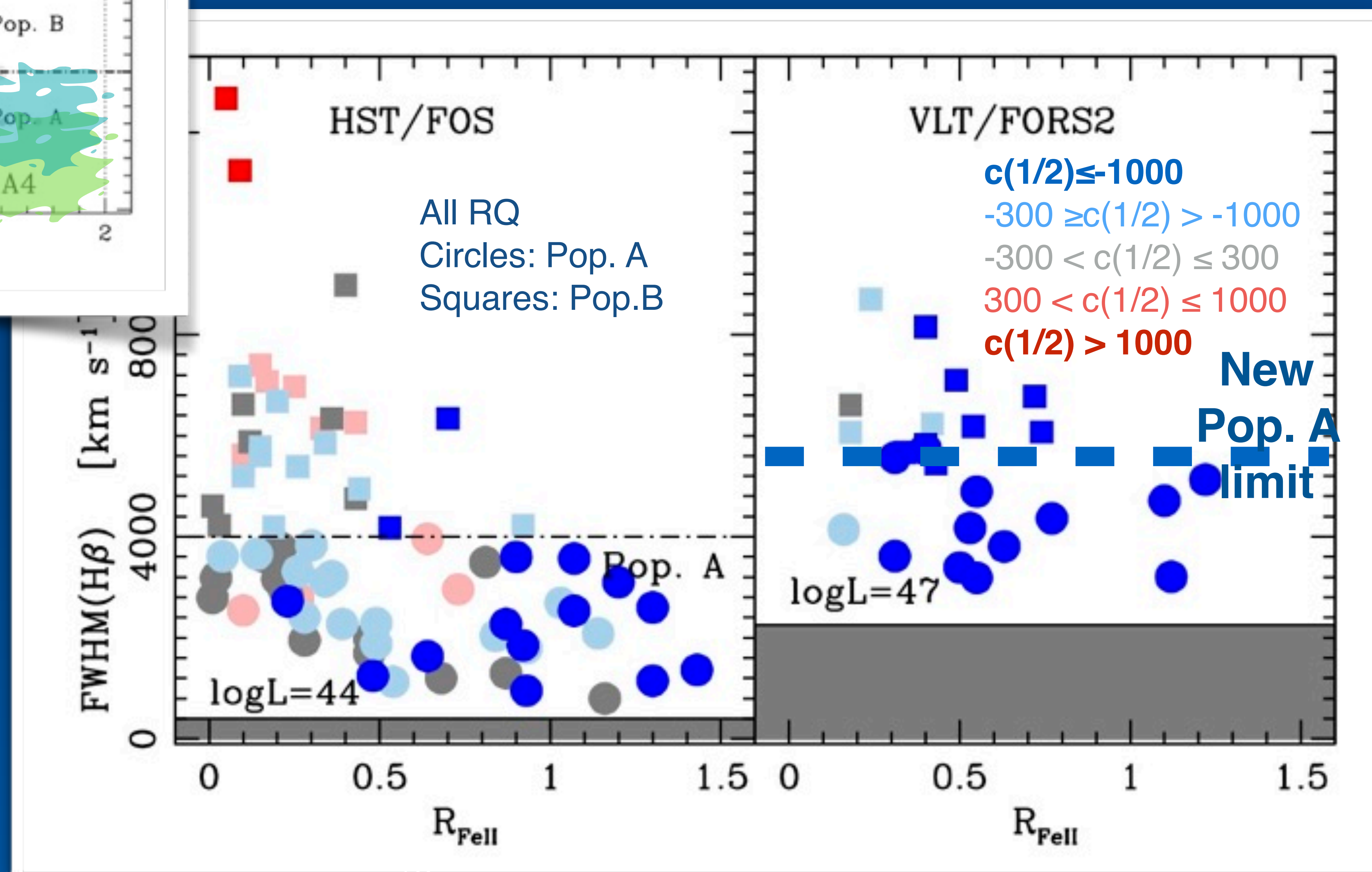


Sulentic et al., 2017

## Virial broadening estimators: CIV vs Hβ FWHM

Low-L:
HST/FOS RQ sample of Sulentic et al.
2007 (CIV, 130 sources)
∩
Marziani et al. 2003 (Hβ, 215)
52 RQ sources

High-L:
VLT/FORS/ISAAC HE sample
28 objects

Same trends seen at low-z (≲1):
**large FWHM CIV/ FWHM Hβ for Pop. A;** rough consistency with large scatter for Pop. B

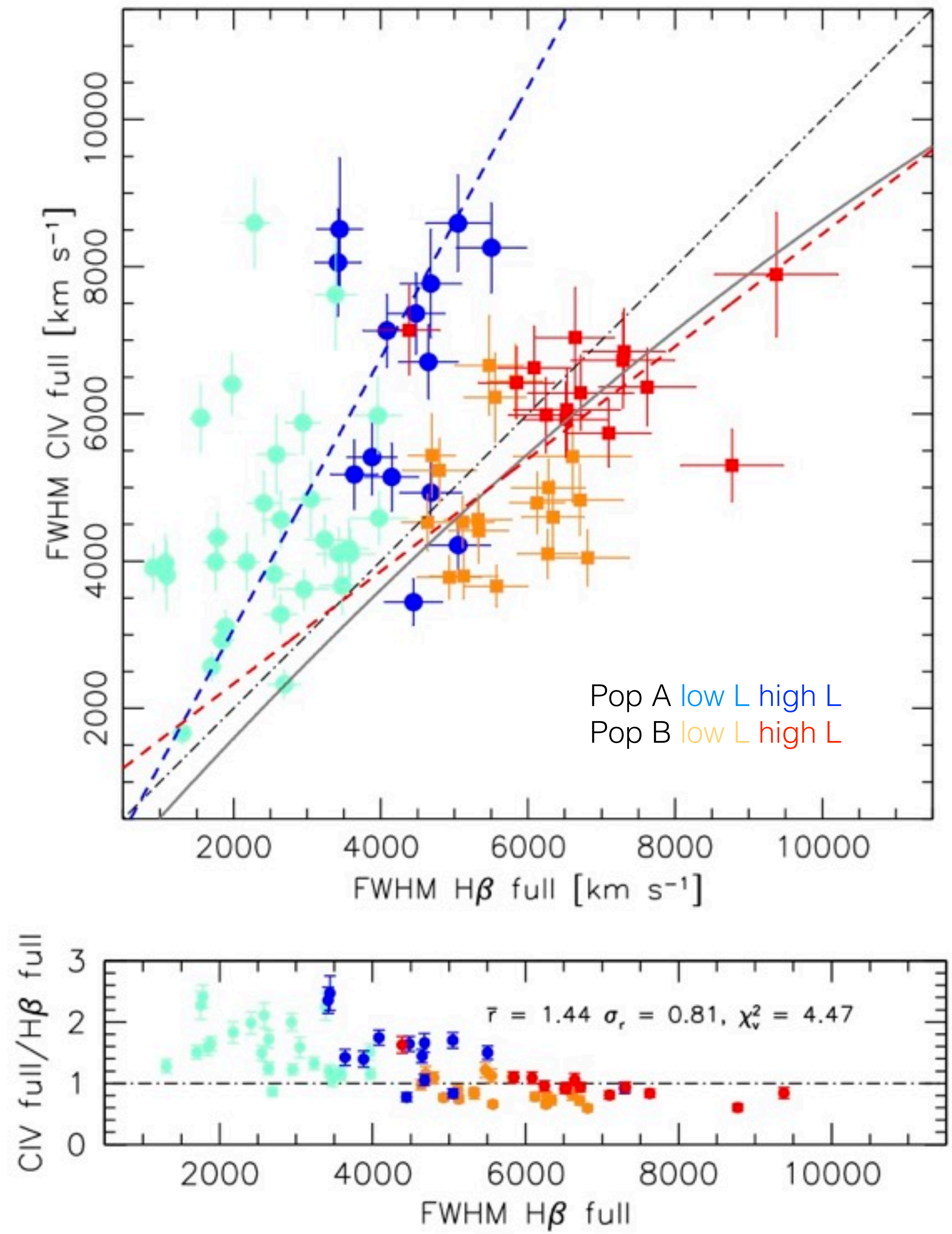

## Virial broadening estimators: the HIL CIVλ1549

# Correlation CIVλ1549 c(1/2) vs. FWHM

# the HIL CIVλ1549 is broadened by a blueshifted excess

c(½) CIVλ1549

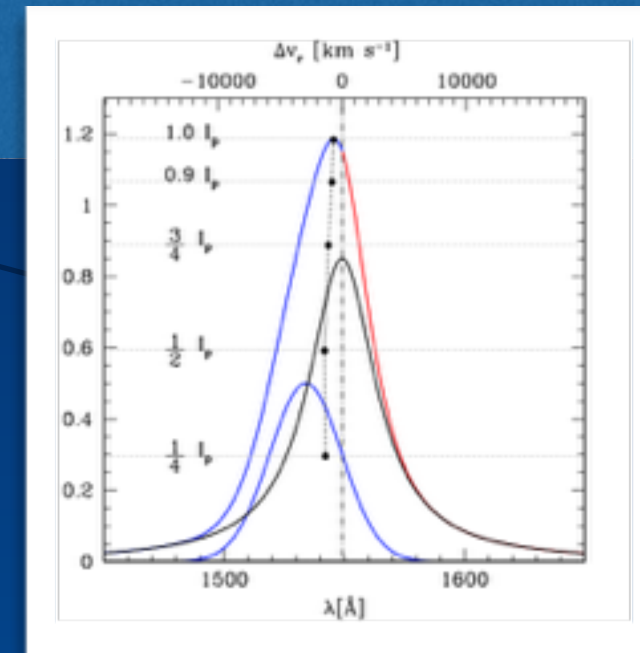


Increase in FWHM(CIVλ1549) associated with a blueshifted component

low *z* sample UV FOS data (130) +HE high L sample (28, red)

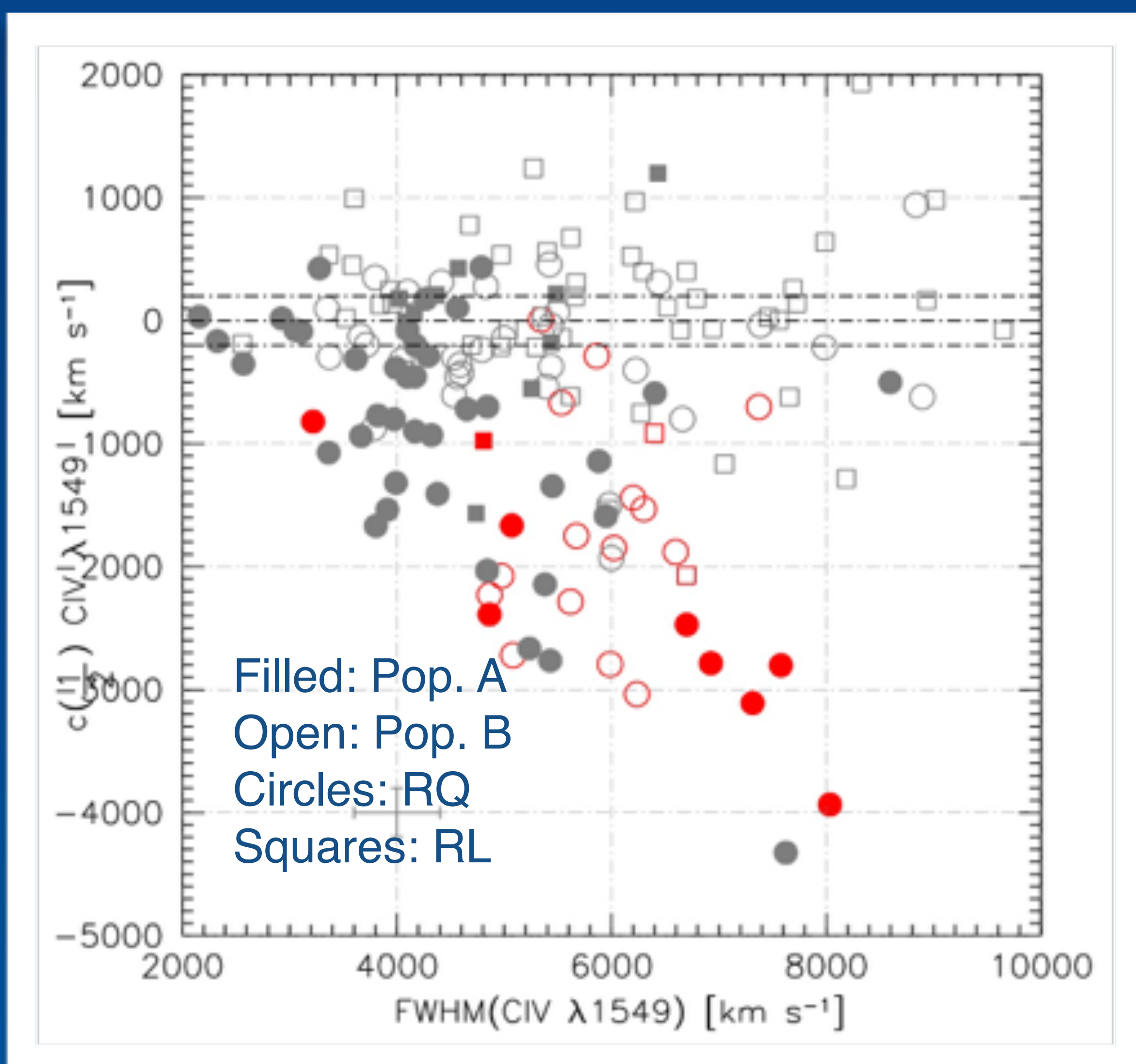


Pop. A RQ only

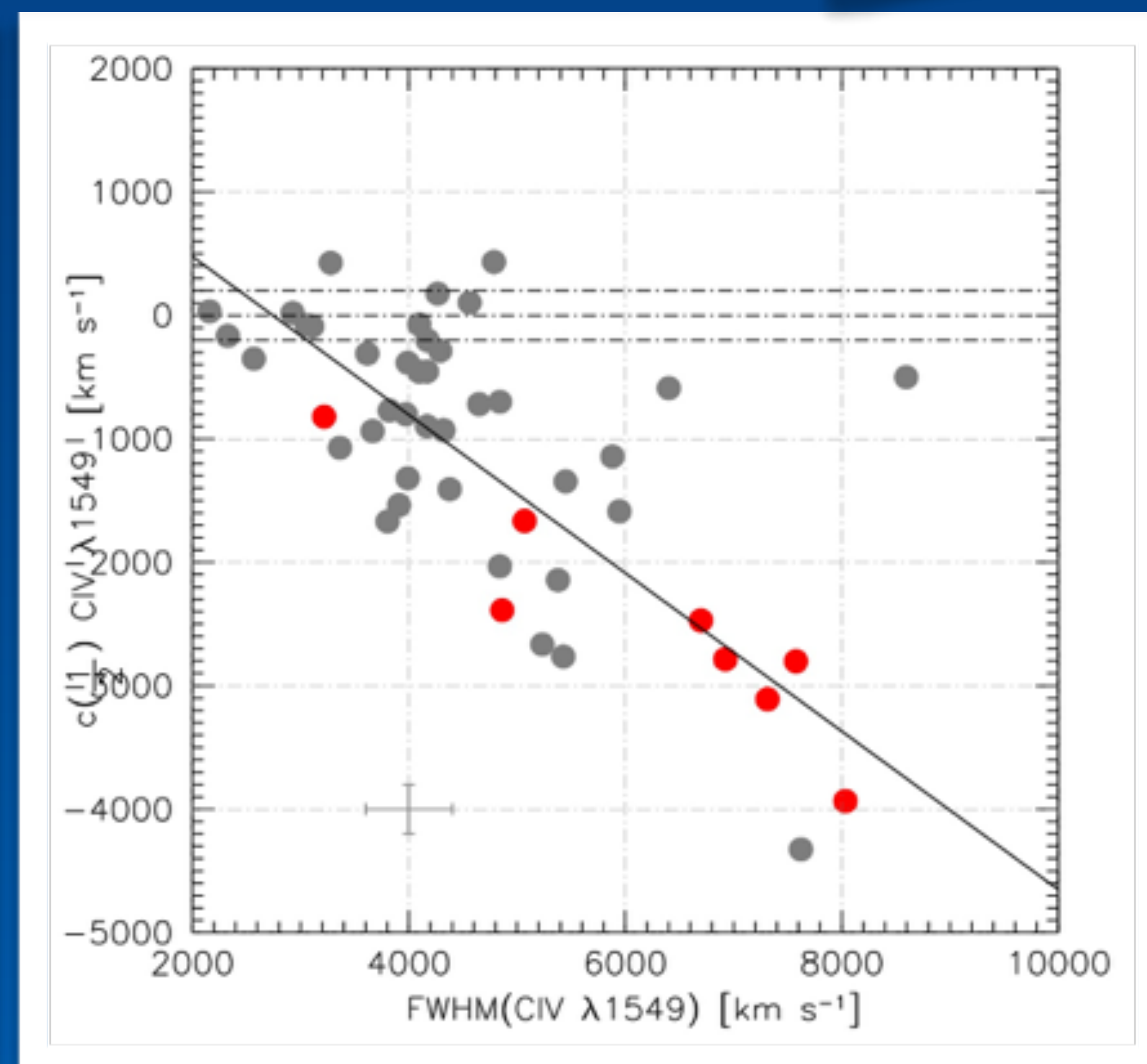


Coatman et al. 2017; Sulentic et al. 2017, Sulentic et al. 2007

Worrisome implications for $M_{BH}$ estimates from CIVλ1549 FWHM

# Virial broadening estimators: HIL CIV corrections

Scaling law that assumes $M_{BH} \propto$ FWHM$^{0.5}$: accounts for the over-broadening of Pop. A sources, but overcorrects for Pop. B.

Correction dependent on $L/L_{Edd}$ or a proxy such as the SiIV+OIV]1400 blend/CIV 1549 ratio: interesting, but not working well on our sample, especially for Pop. B.

Empirical correction based on CIV blueshift: works fairly well for high L sources *only.* Still Requires knowledge of the rest frame.

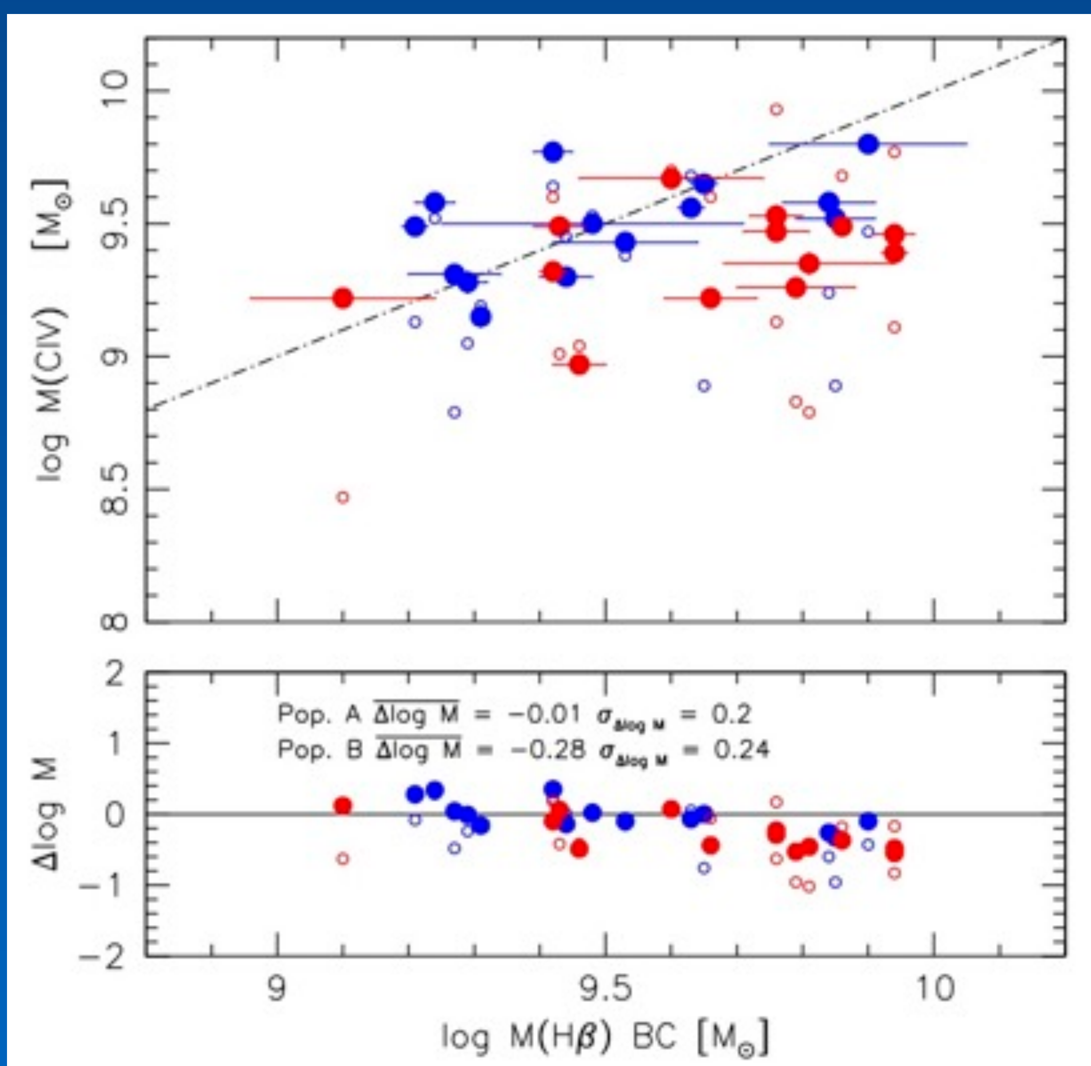


Shen & Liu 2012; Park et al. 2013; Coatman et al. 2016; 2017; Brotherton et al. 2015

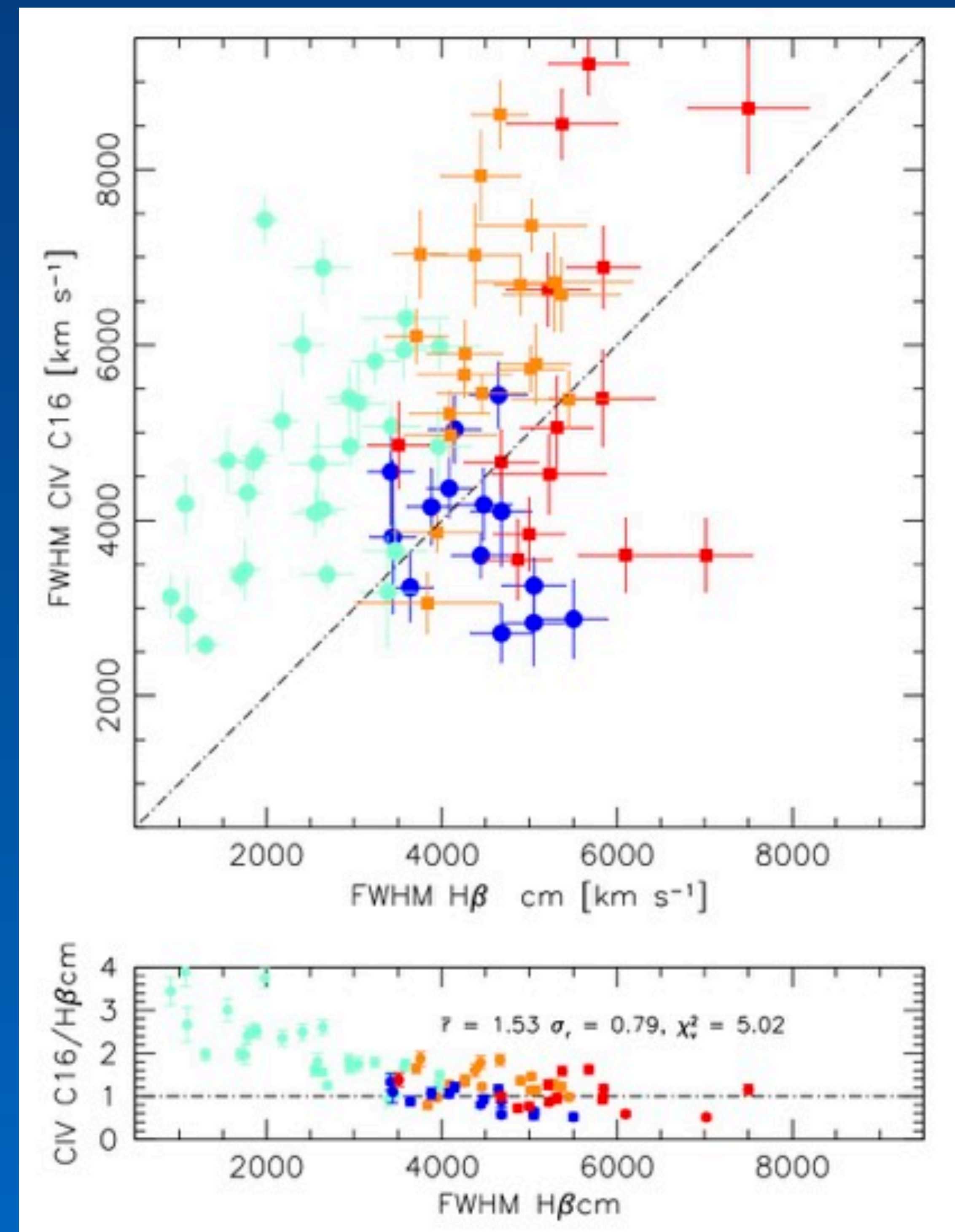

# Virial broadening estimators: HIL CIV corrections

**A threshold in CIV *shift amplitude (c(1/2))* and *L/L*$_{Edd}$ at *L/L*$_{Edd}$≈0.2**

**Strong correlation with *L/L*$_{Edd}$** if blueshifts are significant (bottom panels)

**Weak but significant correlation with luminosity**:
partial CC c(1/2) — L (*L/L*$_{Edd}$ hidden) significant at about 2σ

Multivariate analysis confirms dependence on both L and L/L$_{Edd}$.

**Blueshift trends are consistent with a radiation-driven outflow**

$$v_{term} \propto v_K \sqrt{\mu \frac{L}{L_{Edd}}} \propto L^{-a/2} M_{BH}^{1/2} \sqrt{\mu \frac{L}{L_{Edd}}}$$

$$\propto L^b \sqrt{\frac{L}{L_{Edd}}} \quad if \quad L^{-a/2} M_{BH}{}^{1/2} \mu^{1/2} \propto L^b$$

where $v_K$ is the Keplerian velocity and μ is the force multiplier; Laor & Brandt 2002

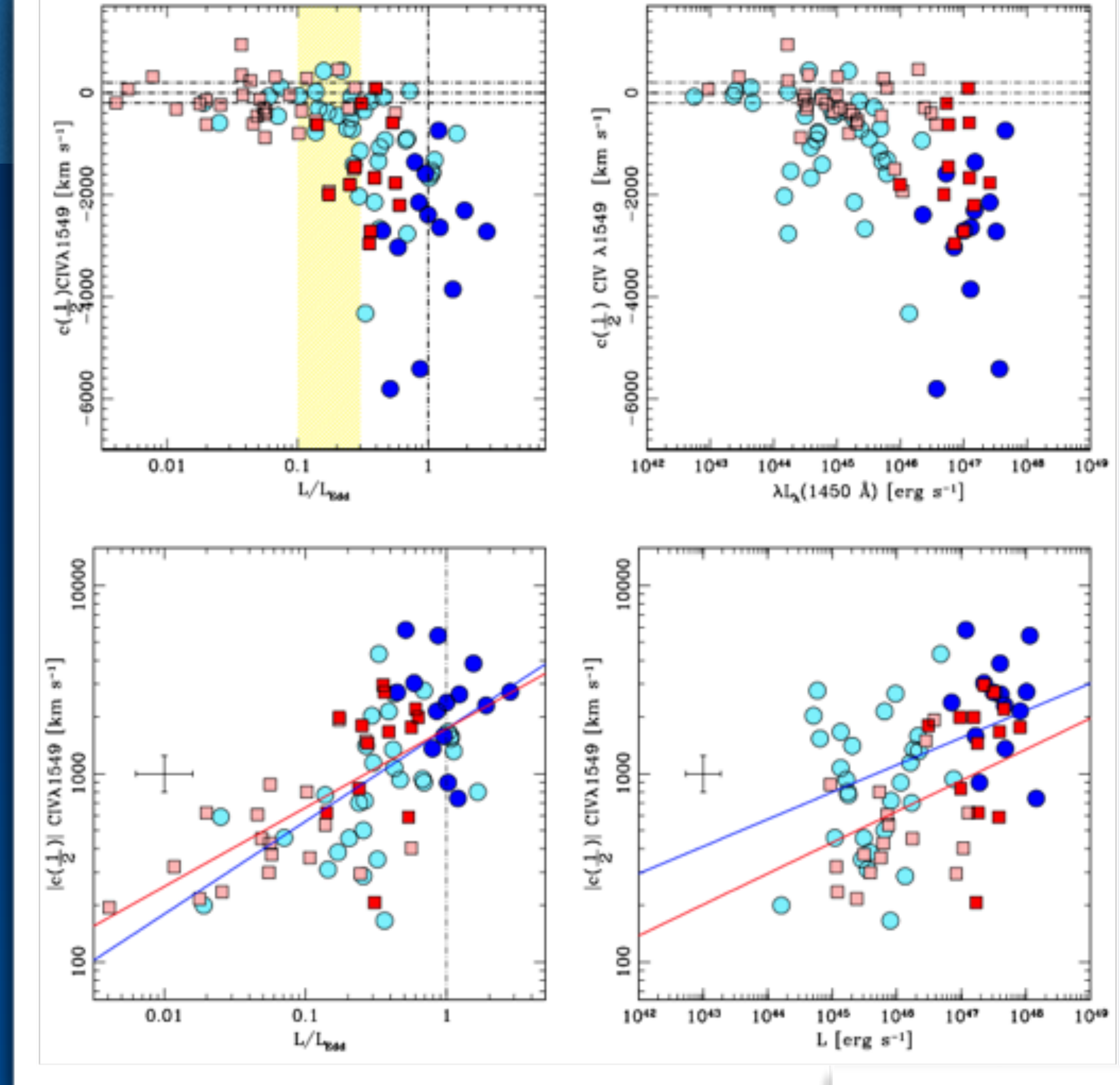


slope a ≈ 0.5 for *L/L*$_{Edd}$;

Circles: Pop. A
Squares: Pop. B

A pure dependence on L arises for *L/L*$_{Edd}$ in a small range.
A strong dependence on *L/L*$_{Edd}$ and a weak dependence on L can be achieved under a variety of scenarios; strength and form of L and *L/L*$_{Edd}$ are sample dependent.

Sulentic et al., 2017

# Virial broadening estimators: HIL CIV corrections

**A correction based on L and c(1/2) reduces scatter, but coefficients are different for Pops. A and B.**

as $\xi_{\rm CIV}$ =FWHM(H$\beta_{\rm BC}$)/FWHM(CIV$\lambda$1549), then

$$\xi_{\rm CIV} = \frac{1}{\beta\left(\alpha - \log \lambda L_\lambda(1450)\right)\cdot\left(\left|\frac{c(\frac{1}{2})}{1000}\right|\right) + \gamma}$$

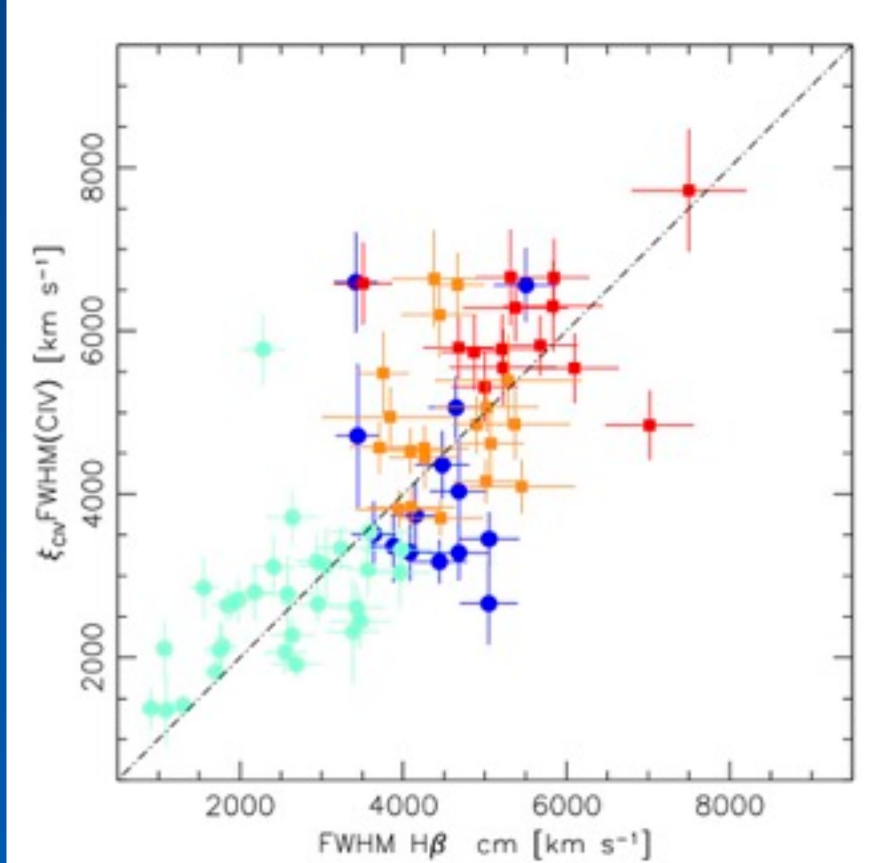


α ≈ −0.347 ± 0.148, β ≈ −0.335 ± 0.083, γ ≈ 1.087 ± 0.09 for Pop. A

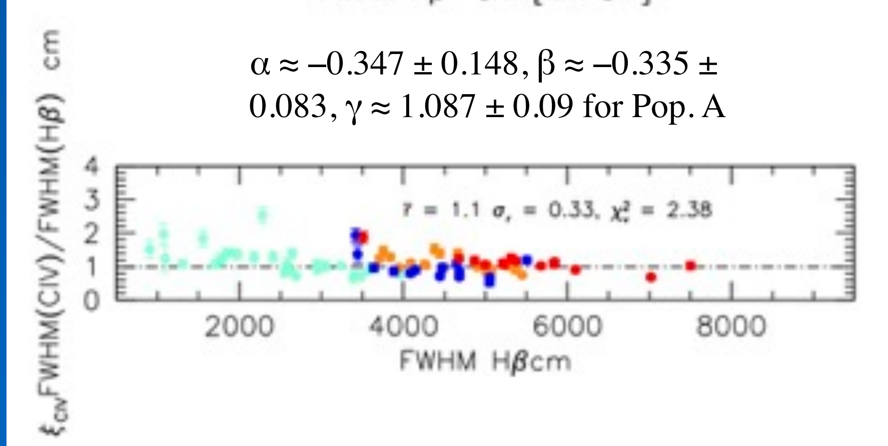


For Pop. B the correction is highly uncertain. A larger sample of Pop. B is needed.

**Corrections based on c(1/2) require rest-frame knowledge.**

A theoretical correction requires that c(1/2) CIV and ionization conditions are accounted for.

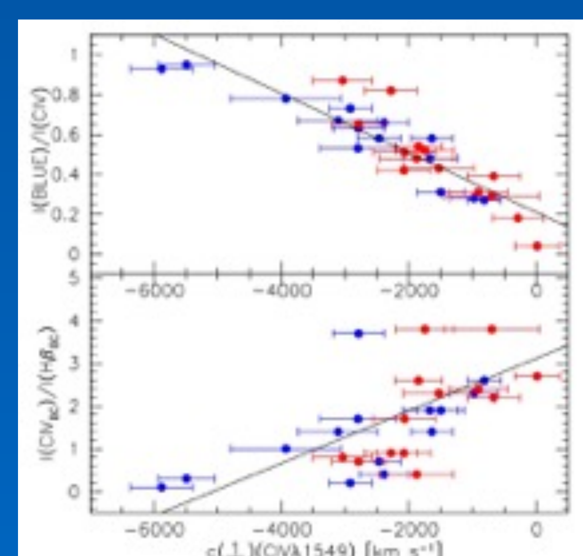

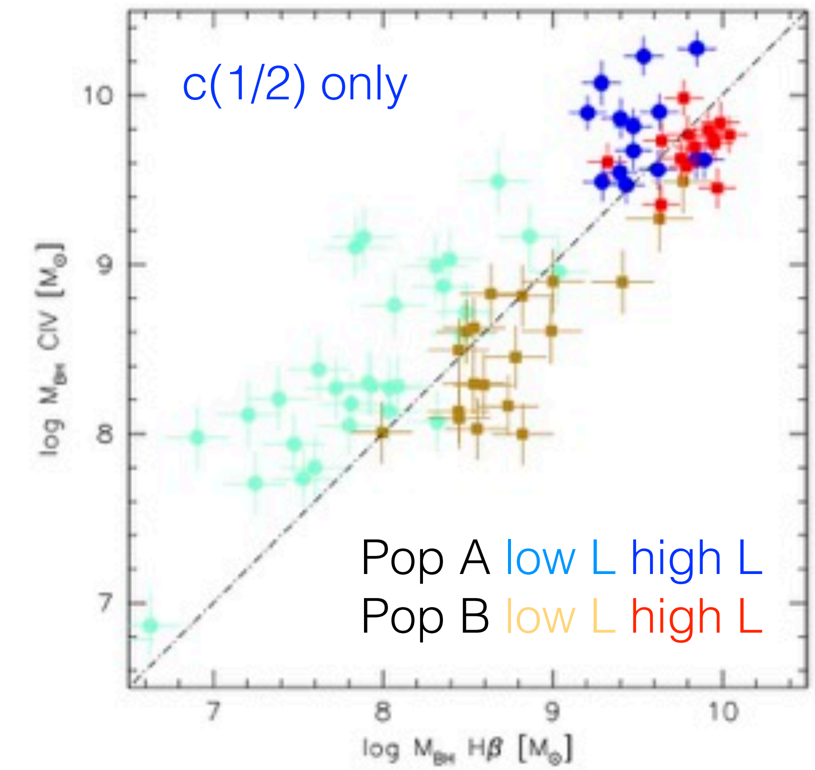


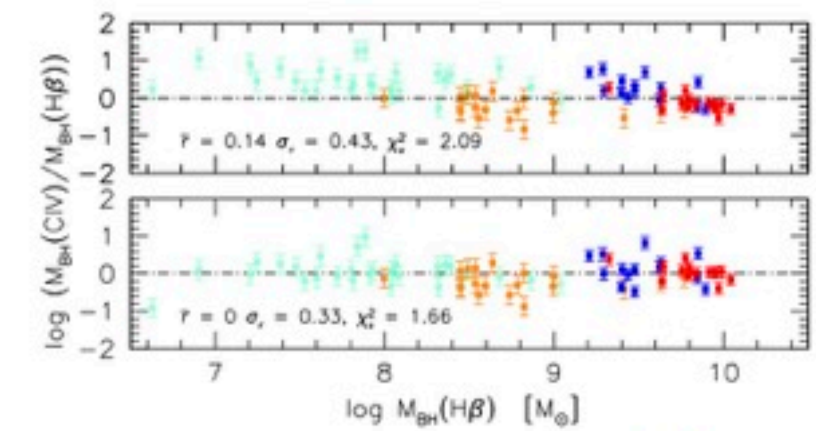


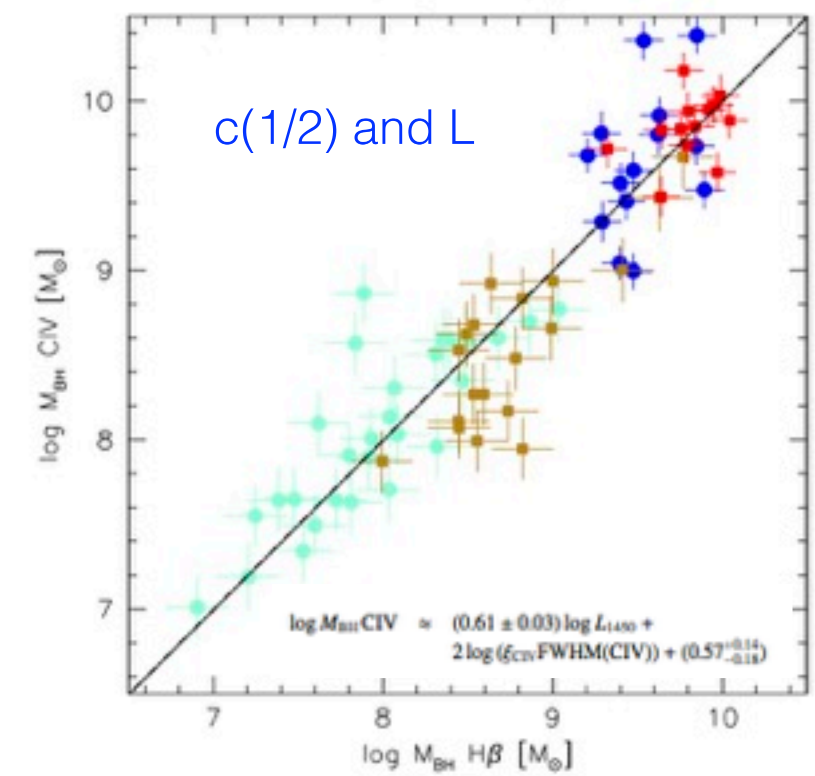

# Virial broadening estimators: HIL CIV corrections —The “Eddington ratio bias”

Sulentic et al. 2015

Selection effects on $L/L_{Edd}$ in flux limited samples

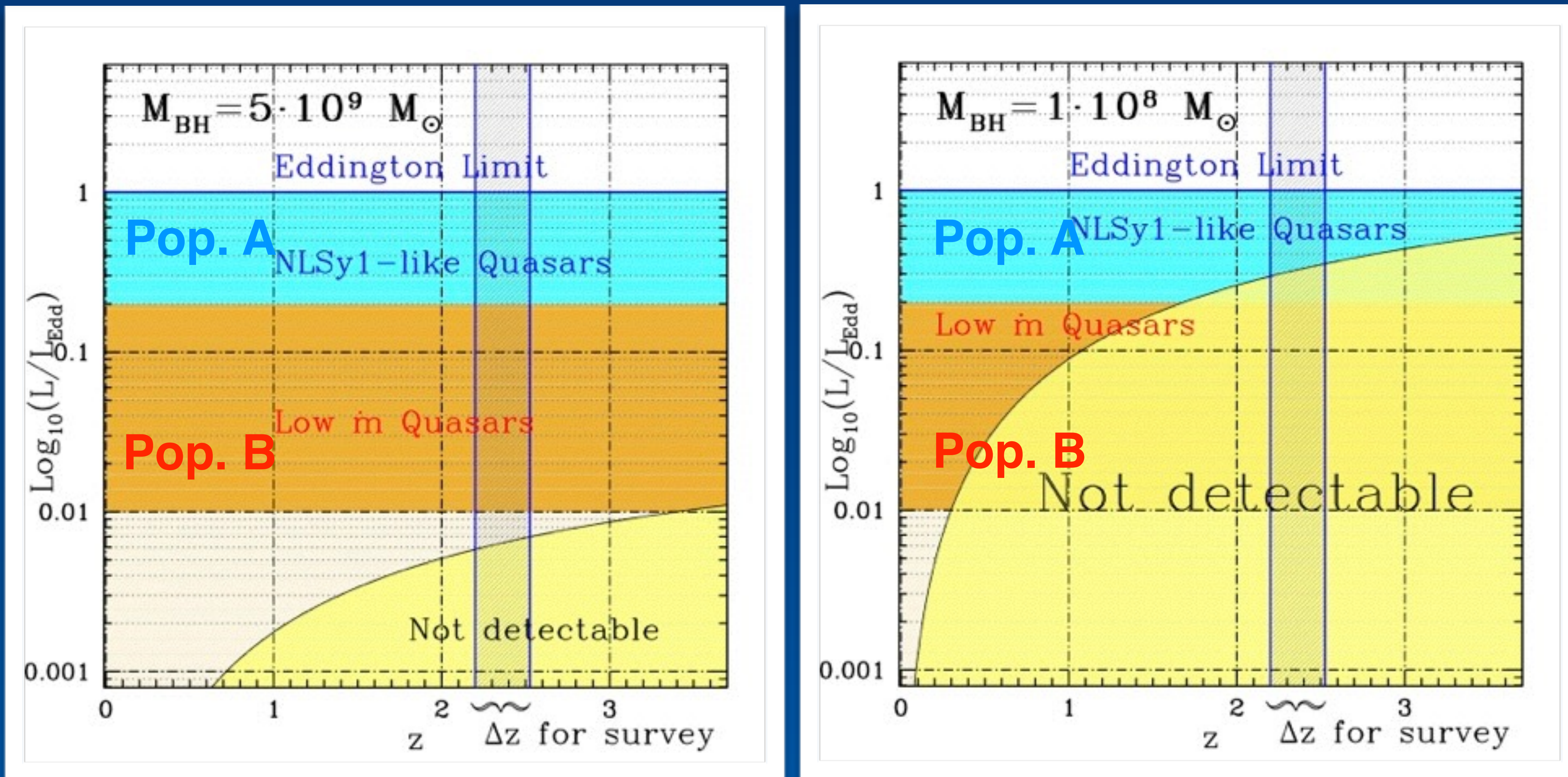


Higher $L/L_{Edd}$ selected at higher *z:* the high frequency of CIV blueshifts associated with an “Eddington ratio” bias.

**$L/L_{Edd}$ (using c(1/2) as a proxy) and *L*-based corrections may remain sample dependent.**

# Virial broadening estimators from IILs: the 1900 Å blend

CIII] measurements have serious problems:
in Pop. A; CIII] faint, blended with FeIII
in Pop. B: affected by VBC.

**FWHM AlIIIλ1860 = FWHM SiIII]λ1892**

**Table 1**
Line Components in the λ1900 Blend

| Ion (1) | λ (Å) (2) | X (eV) (3) | $E_l - E_u$ (eV) (4) | Transition (5) | $A_{ki}$ ($s^{-1}$) (6) | $n_c$ ($cm^{-3}$) (7) |
|---|---|---|---|---|---|---|
| Si II | 1808.00 | 8.15 | 0.000–6.857 | $^2D^o_{3/2} \to {}^2P_{1/2}$ | $2.54 \times 10^6$ | ... |
| Si II | 1816.92 | 8.15 | 0.036–6.859 | $^2D^o_{5/2} \to {}^2P_{3/2}$ | $2.65 \times 10^6$ | ... |
| Al III | 1854.716 | 18.83 | 0.000–6.685 | $^2P^o_{3/2} \to {}^2S_{1/2}$ | $5.40 \times 10^8$ | ... |
| Al III | 1862.790 | 18.83 | 0.000–6.656 | $^2P^o_{1/2} \to {}^2S_{1/2}$ | $5.33 \times 10^8$ | ... |
| [Si III] | 1882.7 | 16.34 | 0.000–6.585 | $^3P^o_2 \to {}^1S_0$ | 0.012 | $6.4 \times 10^4$ |
| Si III] | 1892.03 | 16.34 | 0.000–6.553 | $^3P^o_1 \to {}^1S_0$ | 16700 | $2.1 \times 10^{11}$ |
| [C III] | 1906.7 | 24.38 | 0.000–6.502 | $^3P^o_2 \to {}^1S_0$ | 0.0052 | $7.7 \times 10^4$ |
| C III] | 1908.734 | 24.38 | 0.000–6.495 | $^3P^o_1 \to {}^1S_0$ | 114 | $1.4 \times 10^{10}$ |
| Fe III | 1914.066 | 16.18 | 3.727–10.200 | $z^7P^o_3 \to a^7S_3$ | $6.6 \times 10^8$ | ... |

**FWHM AlIII (anchored to FWHM SiIII]) provides a virial broadening estimator** (but AlIII is a resonant line).

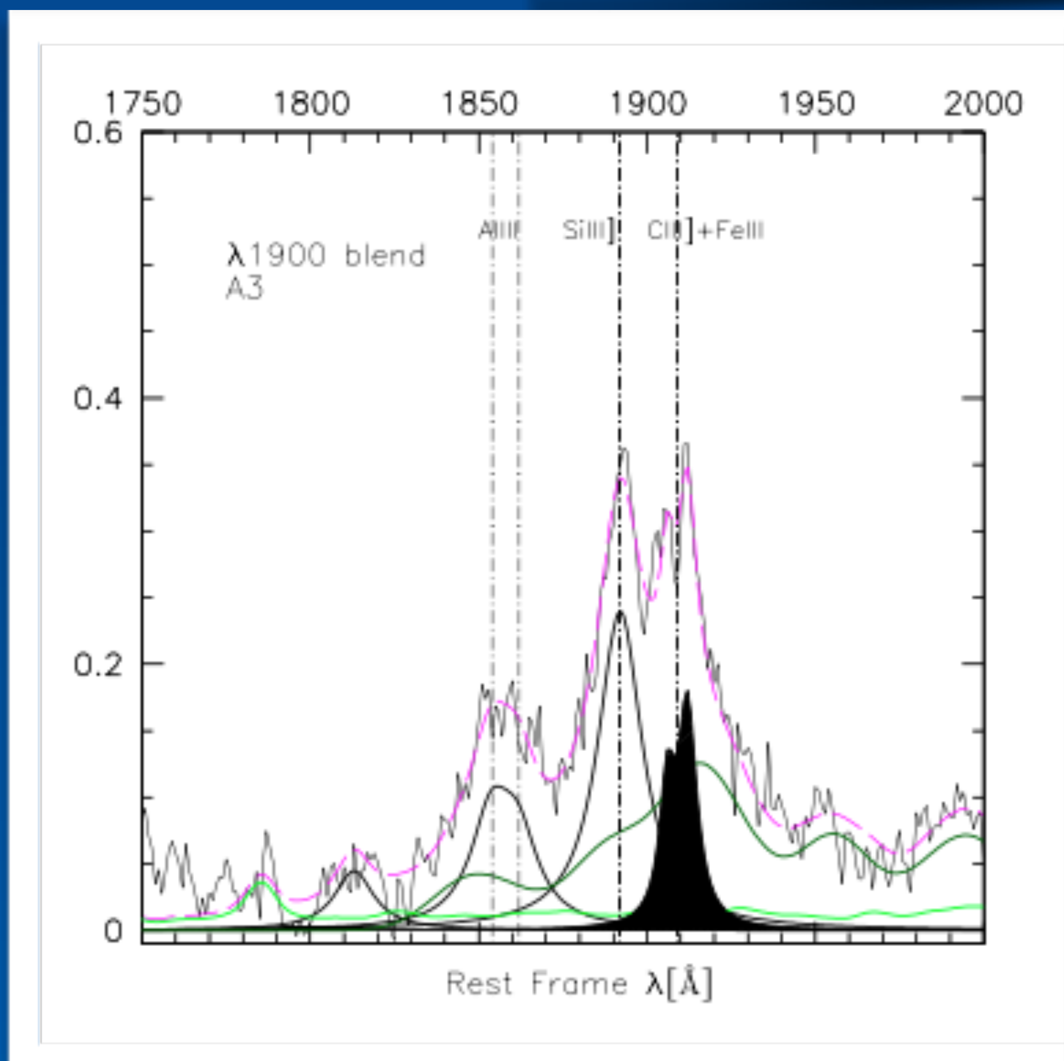


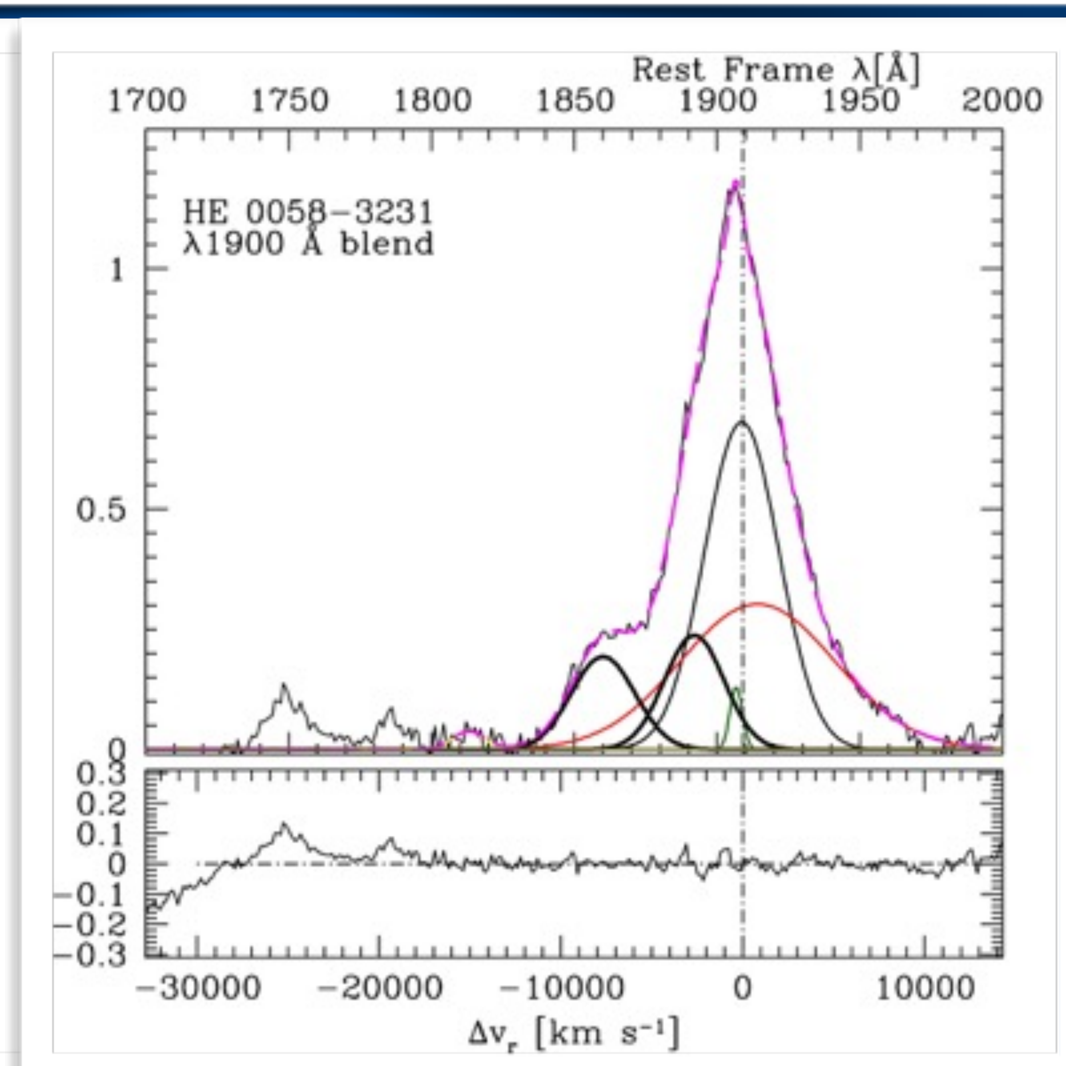

# Virial broadening estimators from IILs: the 1900 Å blend

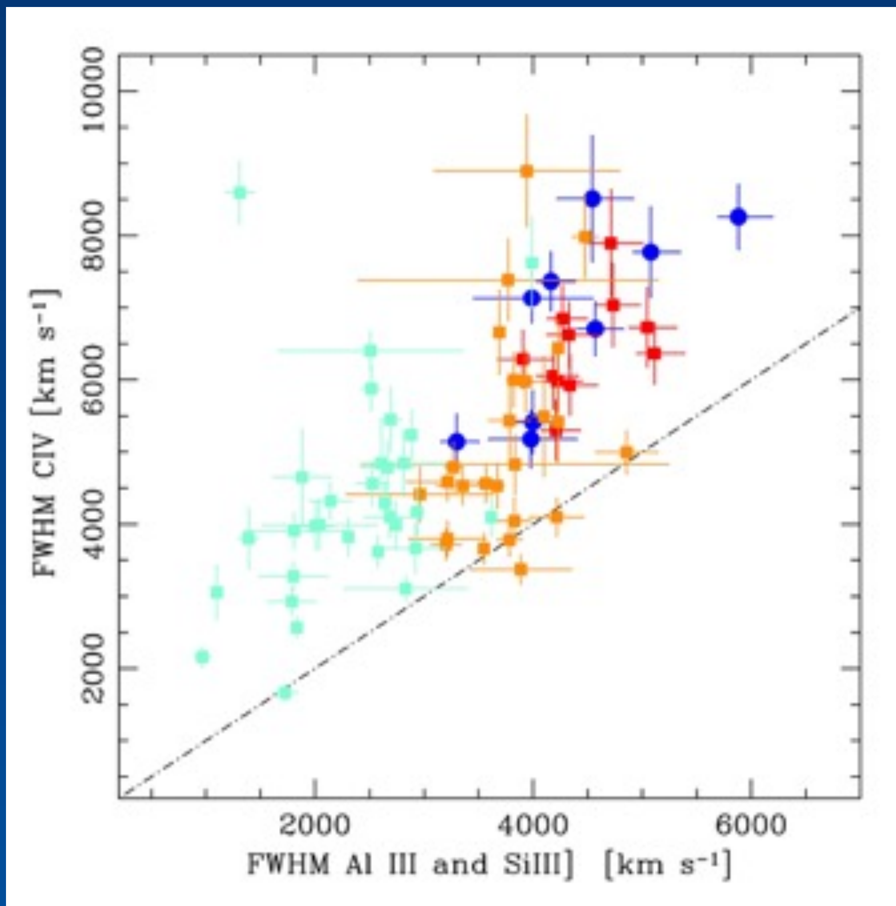


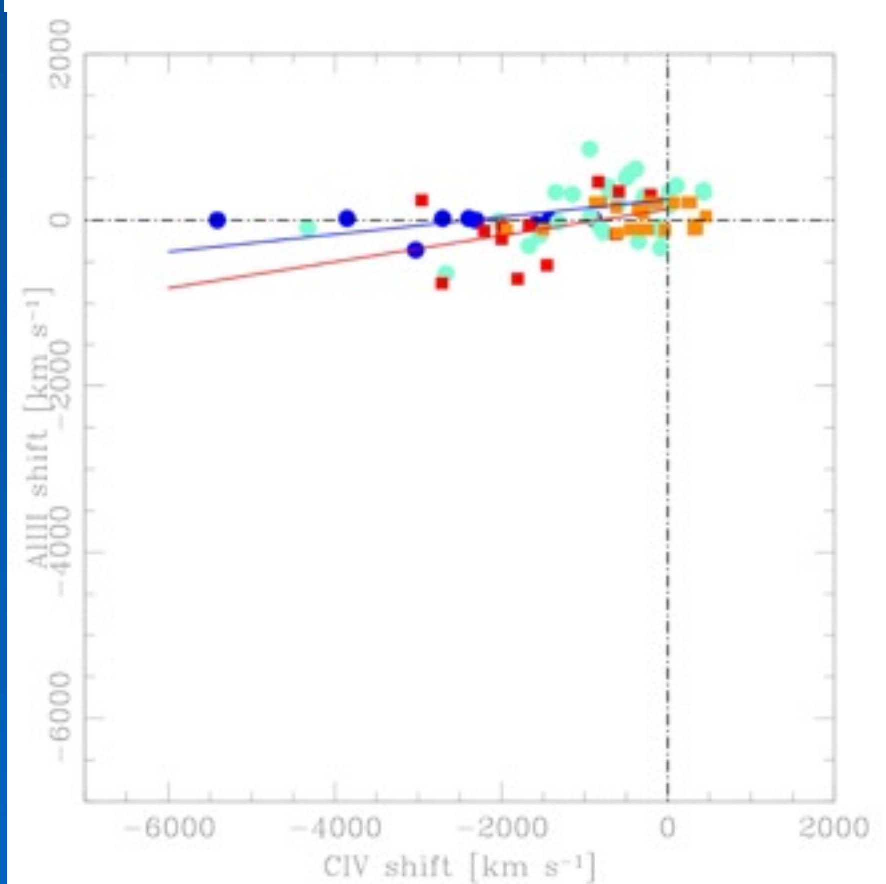


AlIII - SiIII] narrower than CIV, but no clear trend

AlIII shifts < 0.2 CIV shifts; profile is symmetric and (almost) unshifted in most sources.

AlIII - SiIII] relation to CIII]: AlIII broader, but with large scatter

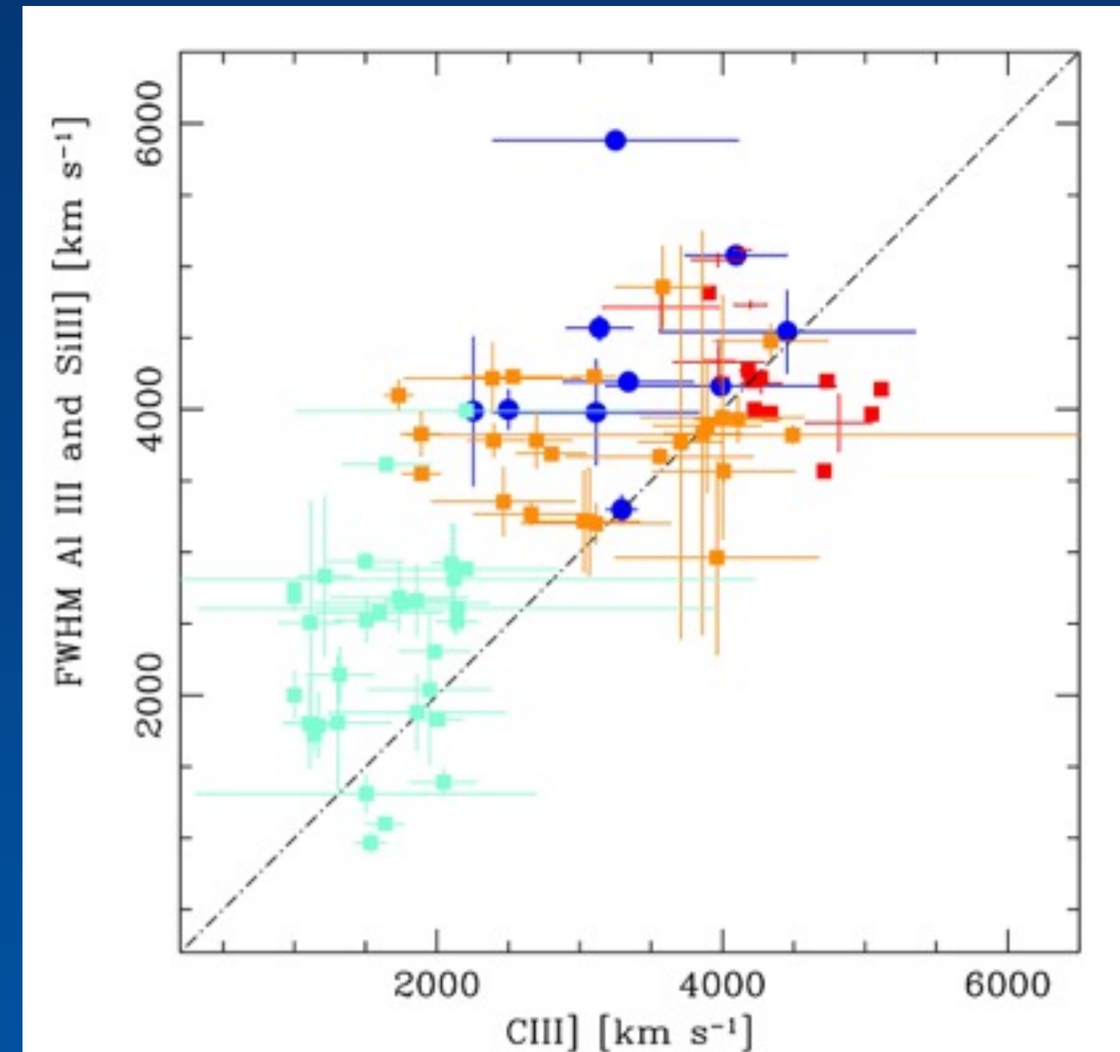


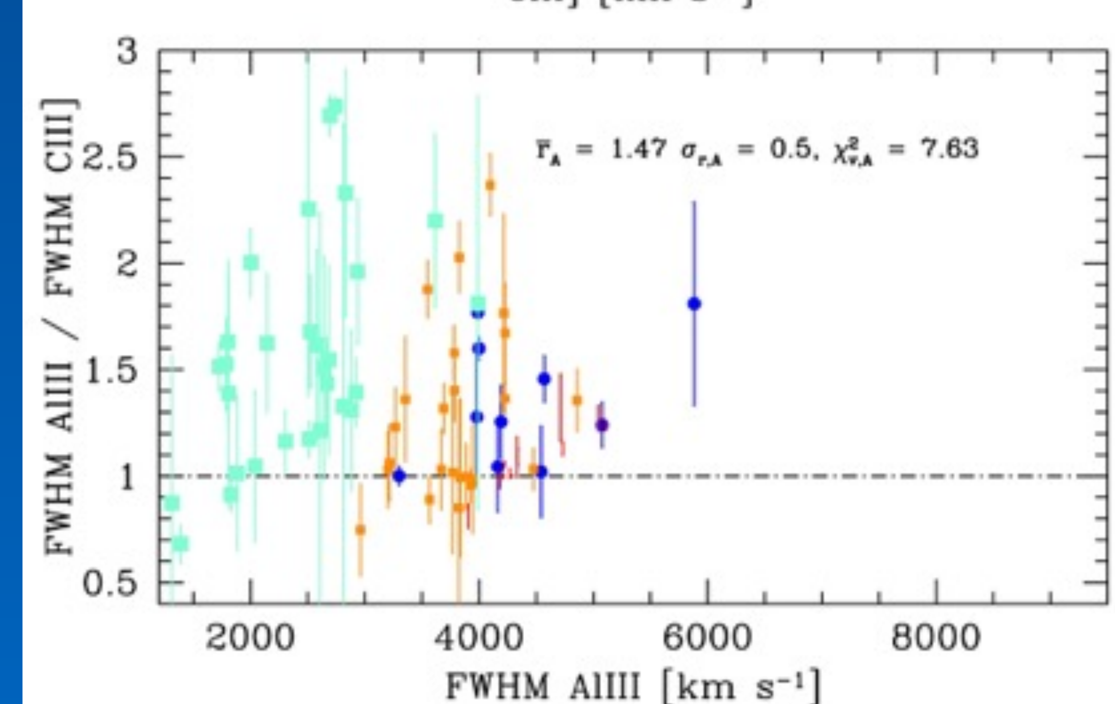

# Virial broadening estimators from IILs: the 1900 Å blend

**Pop. A: very good agreement with Hβ:**
**$\xi_{AlIII}$ = 1.0 (Pop. A)**

**Pop. B: lines are narrower than Hβ:**
**$\xi_{AlIII}$ = 1.35 (Pop. B)**
**$FWHM_{vir}$ = FWHM $H\beta_{BC}$ = 1.35 FWHM $_{AlIII}$**

VBC/BC decomposition choices
creating a small bias

3VBC: med 0.97 SIQR 0.14;
NOVBC (wrong) med 1.05 SIQR 0.13

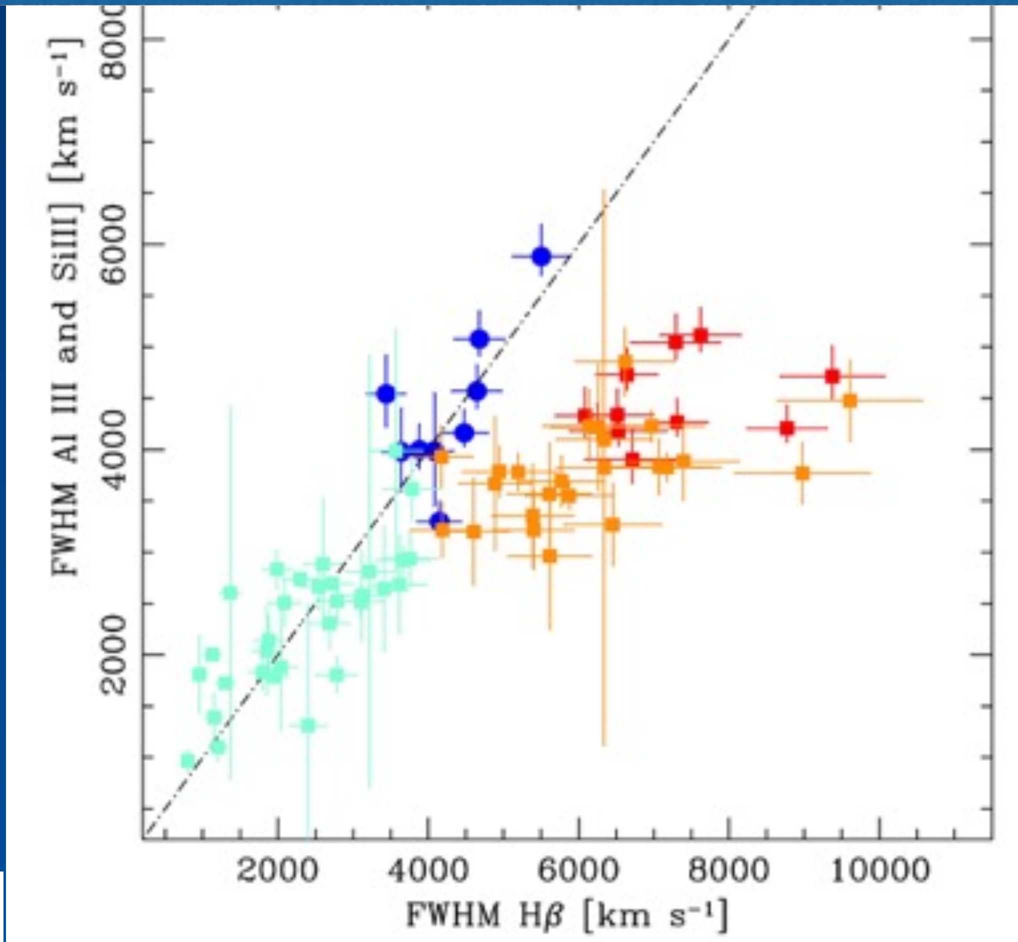


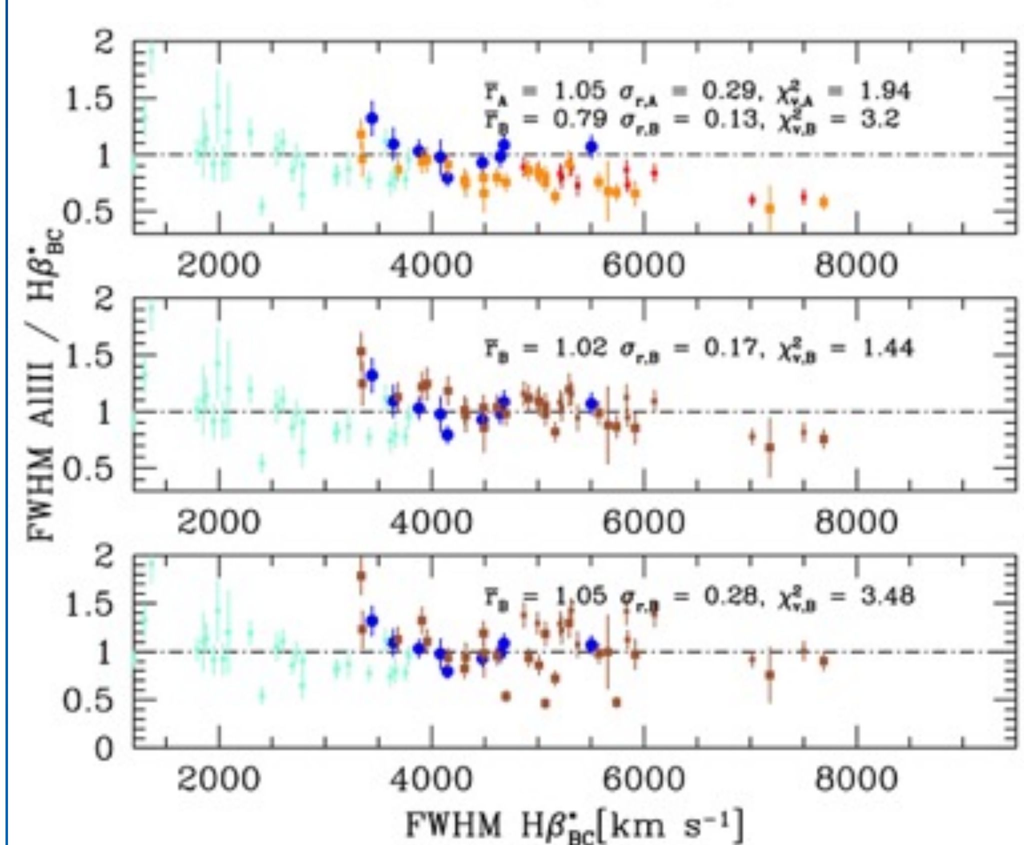


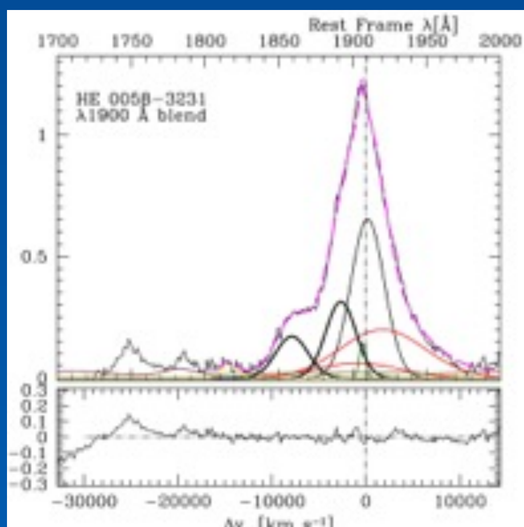


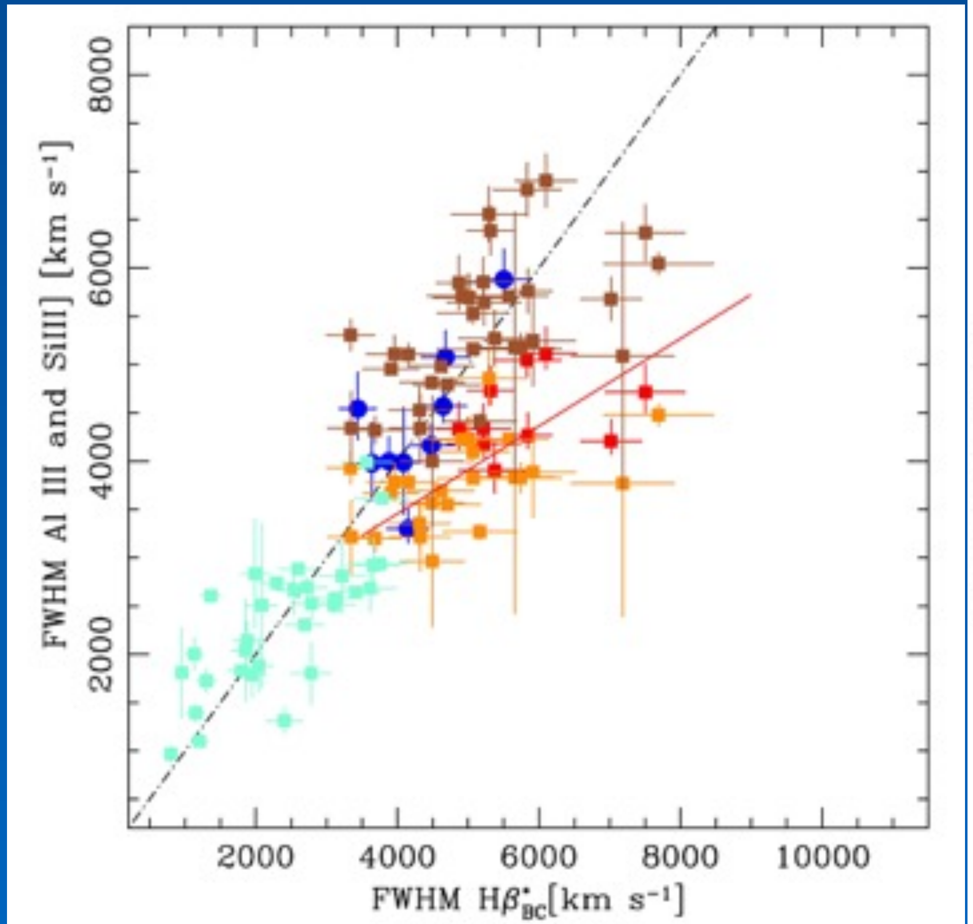


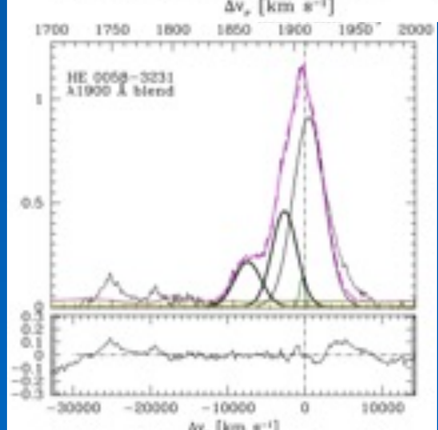

# “Photoioionization” Masses

$$U = \frac{\int_{\nu_0}^{+\infty} \frac{L_\nu}{h\nu} d\nu}{4\pi r_{\mathrm{BLR}}^2 n_\mathrm{e} c}$$

$$r_{\mathrm{BLR}} = \left( \frac{\int_{\nu_0}^{+\infty} \frac{L_\nu}{h\nu} d\nu}{4\pi U n_\mathrm{e} c} \right)^{\frac{1}{2}}$$

$$r_{\mathrm{BLR}} = \underbrace{\frac{1}{(4\pi c)^{\frac{1}{2}}}}_{\mathrm{const.}} \underbrace{(U n_\mathrm{e})^{-\frac{1}{2}}}_{\mathrm{diagnostics}} \left( \underbrace{\int_{\nu_0}^{+\infty} \frac{L_\nu}{h\nu} d\nu}_{\#\ \mathrm{ionizing\ photons}} \right)^{\frac{1}{2}}$$

The photon flux $Un_\mathrm{e}$ is estimated using diagnostic ratios involving AlIII 1860, SiIII] 1892, SiII 1816, CIV 1549, SiIV +OIV] 1400

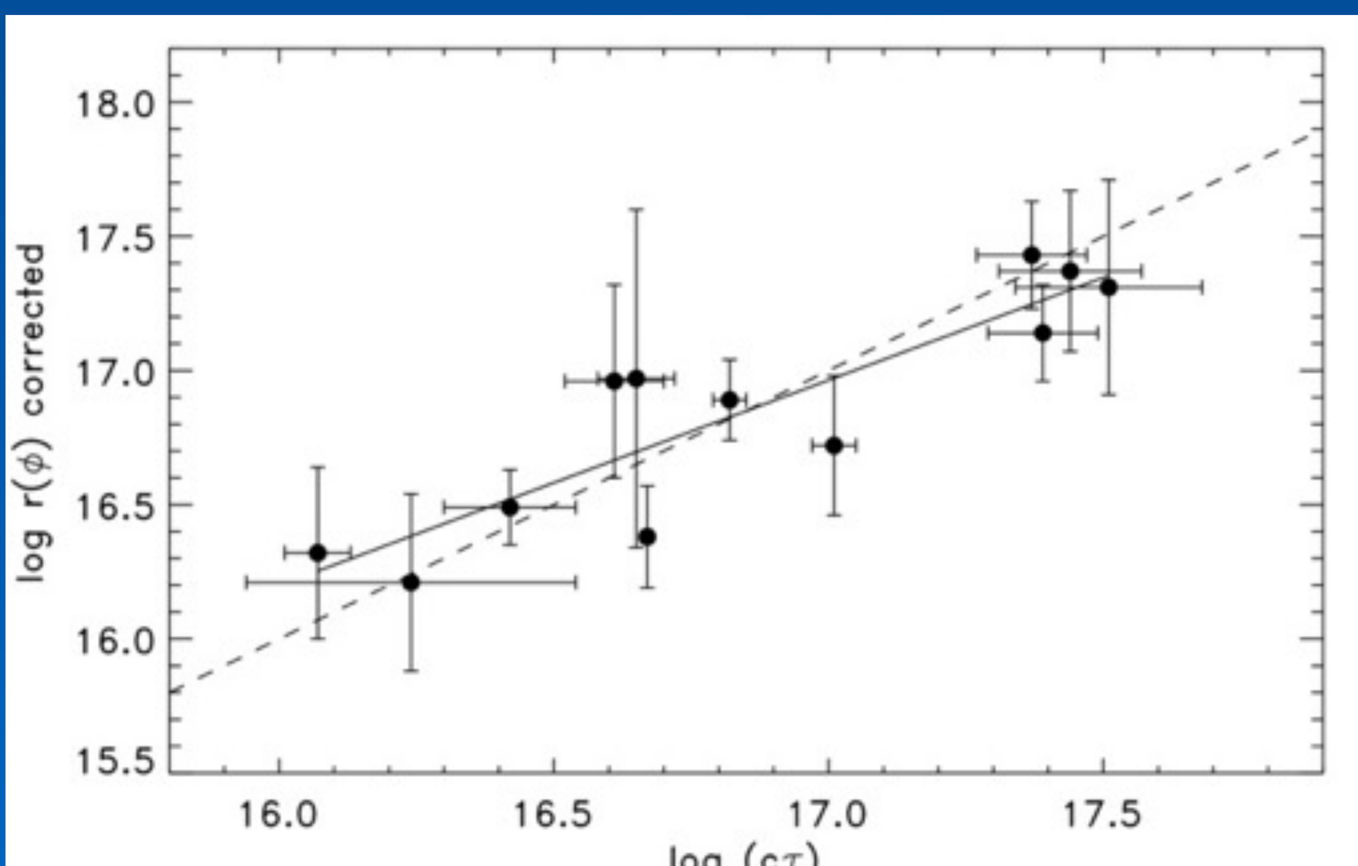


**$r_{\mathrm{BLR}}$ estimates from photo-ionization agree with cτ from RM**

(sample of 12 sources, Negrete et al. 2013)

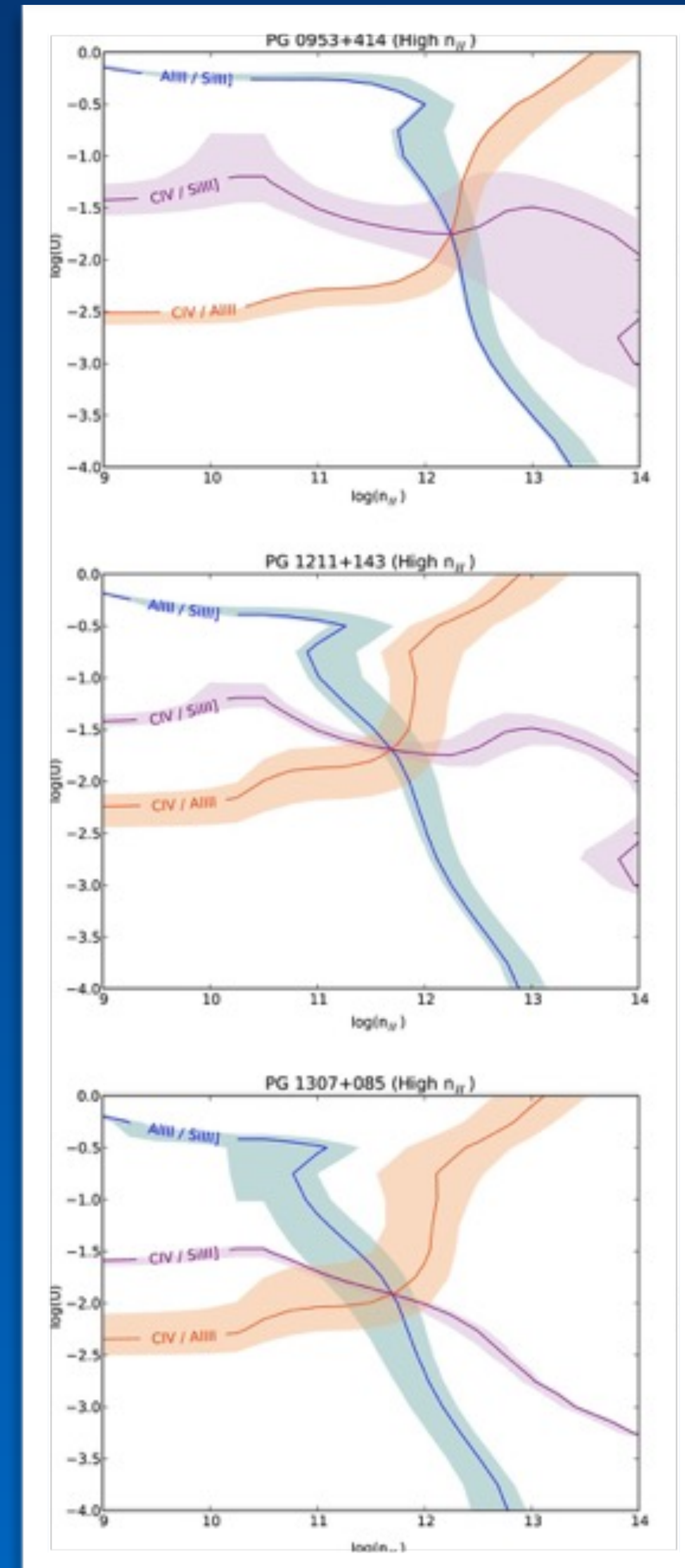

# The photoionization method provides an unbiased estimator of $r_{BLR}$

Both $r_{BLR}$ and $M_{BH}$ estimates at high L remains largely untested

Collin et al. 2006

| | $f(\sigma_{line})$ | $df(\sigma_{line})$ | f(FWHM) | df(FWHM) |
|---|---|---|---|---|
| MEAN SPECTRUM | | | | |
| total | 3.85 | 1.15 | 1.17 | 0.50 |
| Pop1 | 4.20 | 2.09 | 1.81 | 1.38 |
| Pop2 | 3.48 | 1.09 | 0.69 | 0.19 |
| PopA | 3.93 | 1.97 | 2.12 | 1.47 |
| PopB | 3.75 | 1.13 | 0.52 | 0.13 |

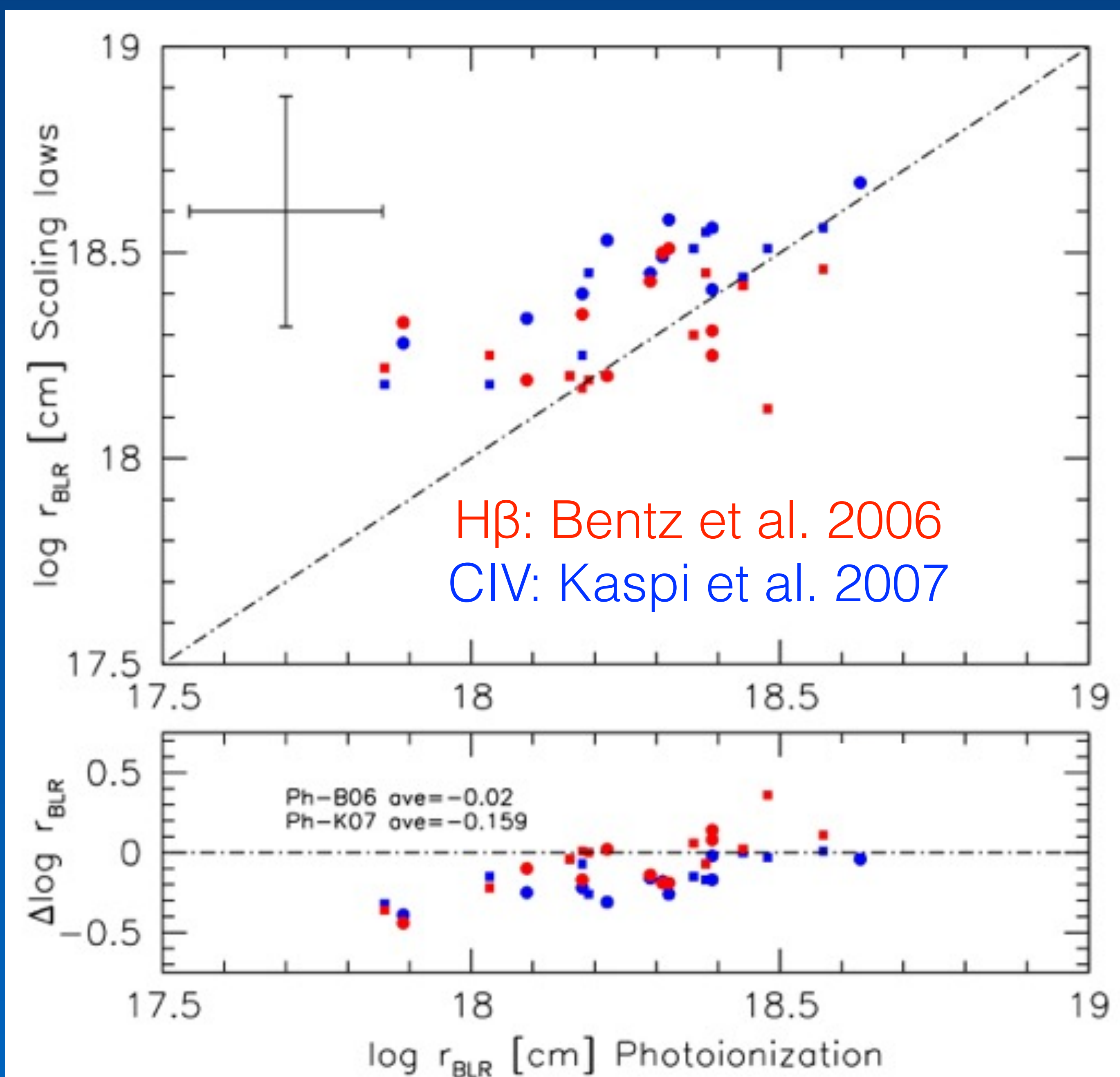


$f$ =1 or different $f$: which is right? We do not know.

$M_{BH}$: the bias emphasizes the role of $f$

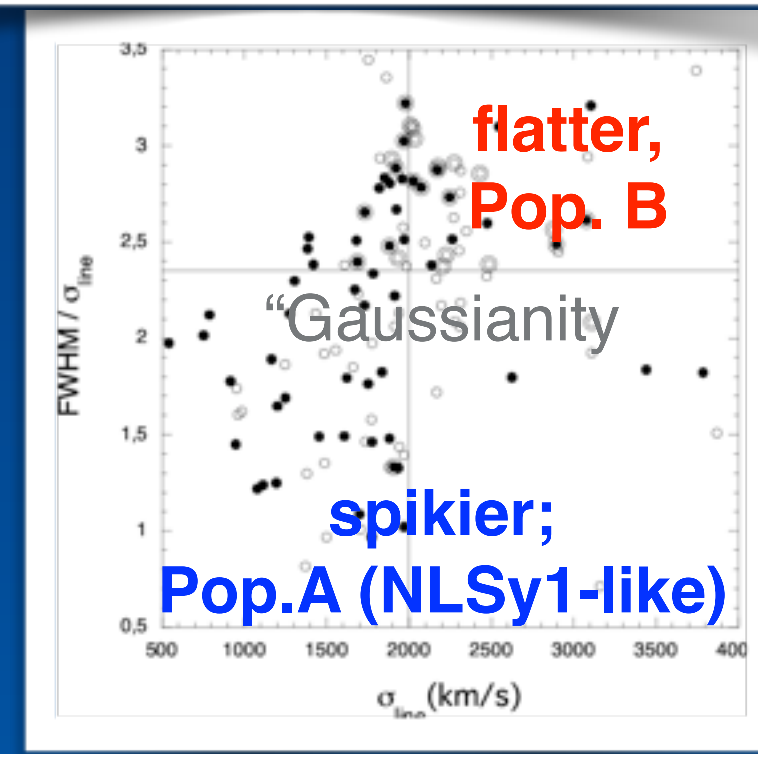


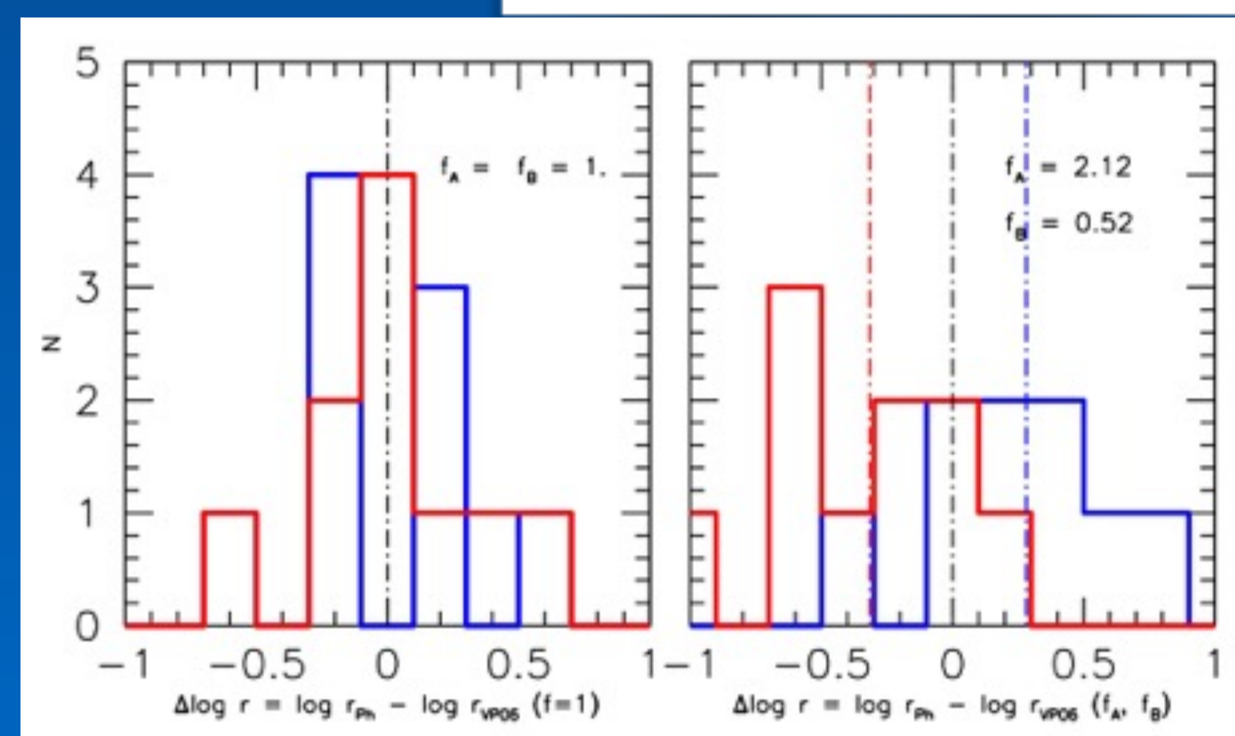

# Conclusion

**Low-ionization lines (Hβ, MgIIλ2800) provide reliable virial broadening estimators** by applying corrections to the observed line width. The corrections depend on the spectral type along the E1 MS, but they are relatively small (less than 20%), and work up to the highest *L* of quasars.

The **HIL CIVλ1549 is not immediately providing a reliable virial broadening estimator.** The profile is broadened by an excess emission on its blue side. The shift amplitude depends on both $L/L_{Edd}$, and *L*. Large shifts are observed in Pop. A, with Eddington ratio above a critical $L/L_{Edd} \sim 0.2$.

**Corrections applied to the observed CIV broadening** remain cumbersome even for Pop. A. Pop. B sources at low Eddington ratio require a different correction (ill defined by the present analysis). They require rest frame determination.

Preliminary result on the 1900 blend indicate that the **IILs lines could provide a better virial broadening estimator than CIV**, even if more data are needed to assess their reliability.

The solution may be to abandon scaling laws altogether and to attempt $M_{BH}$ estimates on an individual basis, considering $r_{BLR}$ from photoionization and $f=f(L/L_{Edd}, a, \theta)$ along the E1 sequence.